

CHAPTER SIX

6. SYNTHETIC STUDY: 1D SOIL MOISTURE PROFILE ESTIMATION

The first step towards estimating the spatial distribution and temporal variation of soil moisture profiles, was the establishment of the profile estimation algorithm (section 3.5) for a one-dimensional soil column. Previous approaches for assimilating observations of near-surface soil moisture content into a hydrologic model (Chapter 3) include: (i) the continuous Dirichlet boundary condition, (ii) hard-updating and (iii) Kalman-filtering. However, there is no consensus as to which approach is the most efficient for soil moisture profile estimation, or on the effect of observation depth and update interval. While application of these assimilation schemes is not new, this chapter identifies: (i) which of the above assimilation schemes is most efficient for soil moisture (and temperature) profile estimation; (ii) the near-surface soil moisture observation depth required for soil moisture profile estimation; (iii) how frequently near-surface soil moisture observations must be made; and (iv) the most important aspects and appropriate form for the hydrologic model to be used in the spatial soil moisture profile estimation problem. The continuous Dirichlet boundary condition is used to illustrate the effects of updating with continuous near-surface soil moisture measurements, as may be available from a single near-surface soil moisture sensor at a weather station.

The governing equations for flow of heat and moisture through unsaturated soil, and the equations relating microwave observations to soil moisture content, are highly non-linear. Therefore the continuous Dirichlet boundary condition and hard-updating assimilation schemes are simpler than the Kalman-filter assimilation scheme, as they allow the non-linear problem to be solved directly. However, with hard-updating, the only way in which near-surface observations can be transferred to deeper layers is through propagation of the near-surface states down the soil profile by the internal physics of the model.

6.1 SYNTHETIC DATA

This chapter uses synthetic soil moisture and temperature data generated from the one-dimensional soil moisture and heat transfer model developed in Chapter 5, to test the soil moisture and temperature profile estimation algorithm. The same soil moisture and heat transfer model was used to both (i) estimate the soil moisture and temperature profile from assimilation of near-surface observations, and (ii) generate the synthetic data sets used for evaluation of the soil moisture and temperature profile estimation algorithm. This allowed testing of the soil moisture and temperature profile estimation algorithm independent of errors in measurement of the soil moisture and temperature profiles, soil properties, and surface fluxes. Furthermore, using the same model to generate the synthetic data as was used in the soil moisture and temperature profile estimation algorithm, eliminated the effects from model errors deriving from neglect of the effects of hysteresis, thermal gradients, heat of wetting and vapour components of the soil heat and moisture balance. The use of synthetic data also allows a broader range of soil and climatic conditions to be investigated than for field data, and allows for greater generalisation in the conclusions.

The soil moisture and heat transfer model developed in Chapter 5 was used to generate 40 days of “true” soil moisture and temperature profiles using the van Genuchten (1980) moisture retention and hydraulic conductivity

Table 6.1: Soil parameters used in evaluation of the soil moisture and temperature profile estimation algorithm.

Total Soil Depth	100 cm
Number of Nodes	31
Soil Thermal and Hydraulic Parameters	Clay Loam
	$K_s = 25 \text{ cm day}^{-1}$
	$\phi = 0.54$
	$\theta_r = 0.2$
	$\eta = 0.008$
	$n = 1.8$
	Proportion of Quartz = 0.03
	Proportion of Other Minerals = 0.41
	Proportion of Organic Matter = 0.02
Initial Conditions	20°C, -50 cm Matric Head

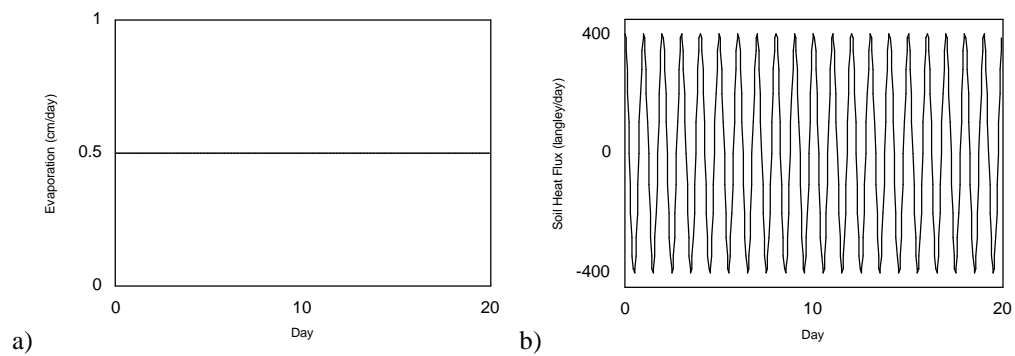


Figure 6.1: Surface boundary conditions: a) moisture flux boundary condition; and b) heat flux boundary condition.

relationships. The soil parameters used by the soil moisture and heat transfer model were those used by Entekhabi *et al.* (1994), Table 6.1.

The “true” soil moisture and temperature profiles were generated by initialising the soil moisture and heat transfer model with the initial conditions of Entekhabi *et al.* (1994), -50 cm matric head and 20°C uniform throughout the 1 m deep soil profile, and subjecting the soil profile to the boundary conditions of Entekhabi *et al.* (1994), 0.5 cm day $^{-1}$ evaporation and a diurnal soil heat flux of 400 langley day $^{-1}$ amplitude at the soil surface (Figure 6.1). The boundary condition at the base of the soil column was zero soil moisture and heat flux.

6.2 KALMAN-FILTER OBSERVATION EQUATION

As thermal infra-red remote sensing observations only provide information about the soil skin temperature, only the soil temperature of the surface node in the soil profile discretisation can be updated. In contrast, remote sensing observations of soil moisture are related to the soil moisture content in a soil layer as thick as a few tenths of the wavelength (Chapter 2 and Chapter 4), and thus provide updating information over a greater depth, being the observation depth.

The simplest way to make a Kalman-filter update of the hydrologic model from Chapter 5, with near-surface soil moisture data from remote sensing observations, is to directly apply the inferred soil matric head over the observation depth d . This eliminates the need for linearisation of the backscattering/brightness temperature, dielectric and water retention models, thus eliminating linearisation errors in the observation equation. This is the *only* way in which model updates

may be made using the hard-updating assimilation scheme. Hence, the Kalman-filtering observation equation (3.3) used in this thesis is

$$\begin{Bmatrix} \psi_1 \\ \psi_2 \\ \vdots \\ \psi_d \\ \vdots \\ \psi_{N-1} \\ \psi_N \\ \hline T_1 \\ T_2 \\ \vdots \\ T_{N-1} \\ T_N \end{Bmatrix} = \begin{bmatrix} 1 & 0 & \cdots & 0 & \cdots & 0 & 0 & \cdots & 0 & 0 & \cdots & 0 & 0 \\ 0 & 1 & \cdots & 0 & \cdots & 0 & 0 & \cdots & 0 & 0 & \cdots & 0 & 0 \\ \vdots & \vdots & \ddots & \vdots & \ddots & \vdots & \vdots & \vdots & \ddots & \vdots & \vdots & \vdots & \vdots \\ 0 & 0 & \cdots & 1 & \cdots & 0 & 0 & \cdots & 0 & 0 & \cdots & 0 & 0 \\ \hline 0 & 0 & \cdots & 0 & \cdots & 0 & 0 & \cdots & 1 & 0 & \cdots & 0 & 0 \end{bmatrix} \begin{Bmatrix} \psi_1 \\ \psi_2 \\ \vdots \\ \psi_d \\ \vdots \\ \psi_{N-1} \\ \psi_N \\ \hline T_1 \\ T_2 \\ \vdots \\ T_{N-1} \\ T_N \end{Bmatrix} + (\mathbf{v}) \quad (6.1),$$

where T_1 is the surface soil temperature from thermal infra-red observations and ψ_d is the soil matric suction at the observation depth. Writing the observation equation in this form makes the soil moisture and temperature profile estimation algorithm using the Kalman-filter assimilation scheme extremely versatile, as it allows for updating to be undertaken for either: (i) direct measurements of near-surface soil moisture content or; (ii) by inverting any algorithm which relates near-surface soil moisture content to remote sensing observations. This is a key difference from the Kalman-filter study presented by Entekhabi *et al.* (1994), which linearised the brightness temperature model (2.15) of Njoku and Kong (1977).

6.3 INITIALISATION PHASE

The one-dimensional soil moisture and heat transfer model from Chapter 5 was initialised with the same poor initial guess used by Entekhabi *et al.* (1994), matric head of -300 cm and soil temperature of 15°C uniform throughout the soil profile. The initial profile conditions are illustrated in Figure 6.2.

The same model parameters, boundary conditions and initial profiles as in Entekhabi *et al.* (1994), were used to replicate their situation for comparison. It is then possible to comment on the form of the observation equation used in this

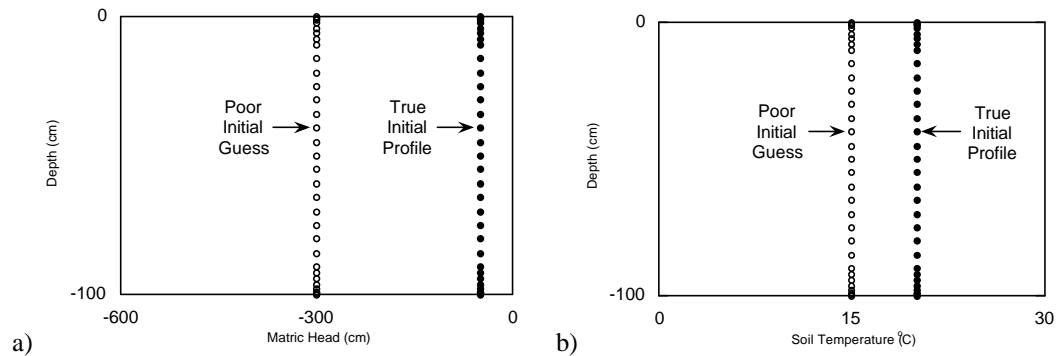


Figure 6.2: Initial profile conditions: a) soil moisture; and b) soil temperature.

study, and contrast it to the linearisation of the brightness temperature model used in Entekhabi *et al.* (1994).

6.4 DYNAMIC PHASE

Upon initialisation with the poor initial guess of the soil moisture and temperature profiles, the dynamic modelling phase was commenced (section 3.5.2). In this phase, the same boundary conditions as used for generating the “true” soil moisture and temperature profiles were applied. The one-dimensional soil moisture and heat transfer model was then updated with near-surface “observations” (taken from the “true” profile simulations) for various soil moisture observation depths and updating frequency, using the various assimilation schemes. This allowed evaluation of the assimilation schemes efficiency, and assessment of the effect from observation depth and update frequency on profile estimation.

6.4.1 CONTINUOUS DIRICHLET BOUNDARY CONDITION

The continuous Dirichlet boundary condition is where the boundary node(s) are held at a known value for a specified period. When the simulated near-surface soil states are updated using either the hard-update or Kalman-filter assimilation schemes, the model estimate of the states in the near-surface soil layers are replaced with the observations, and the information contained in these observations is transferred to deeper depths through the physics of the model. Thus, these updating approaches are in some degree similar to the continuous

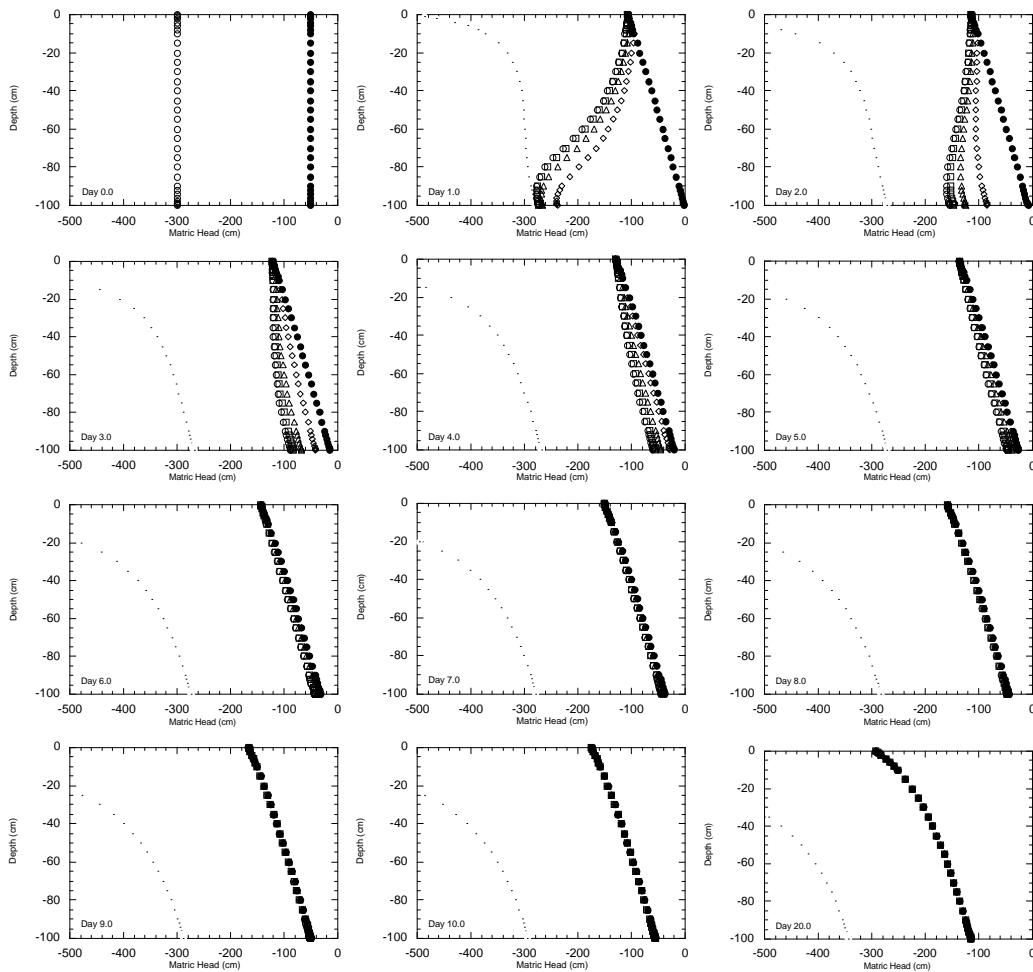


Figure 6.3: Comparison of soil moisture profile estimation using the continuous Dirichlet boundary condition for observation depths of 0 (open circle), 1 (open square), 4 (open triangle) and 10 cm (open diamond) with the “true” soil moisture profile (solid circle) and the open loop soil moisture profile (open circle with dot).

Dirichlet boundary condition, at least for the period during which the updated surface node(s) remain close to the observation.

To identify how much of the profile estimation was a result of the actual updating of the model and how much was a result of the continuous Dirichlet boundary condition, a continuous Dirichlet boundary condition was applied to the near-surface soil nodes for various observation depths. For the soil moisture equation, the Dirichlet boundary condition was applied to depths of 0 (surface node), 1, 4 and 10 cm, while for the temperature equation, the Dirichlet boundary condition was applied only to the surface node. Observations over a depth of 1 cm would be representative of what can be achieved from most current remote sensing systems, whilst 10 cm represents the maximum observation depth that is

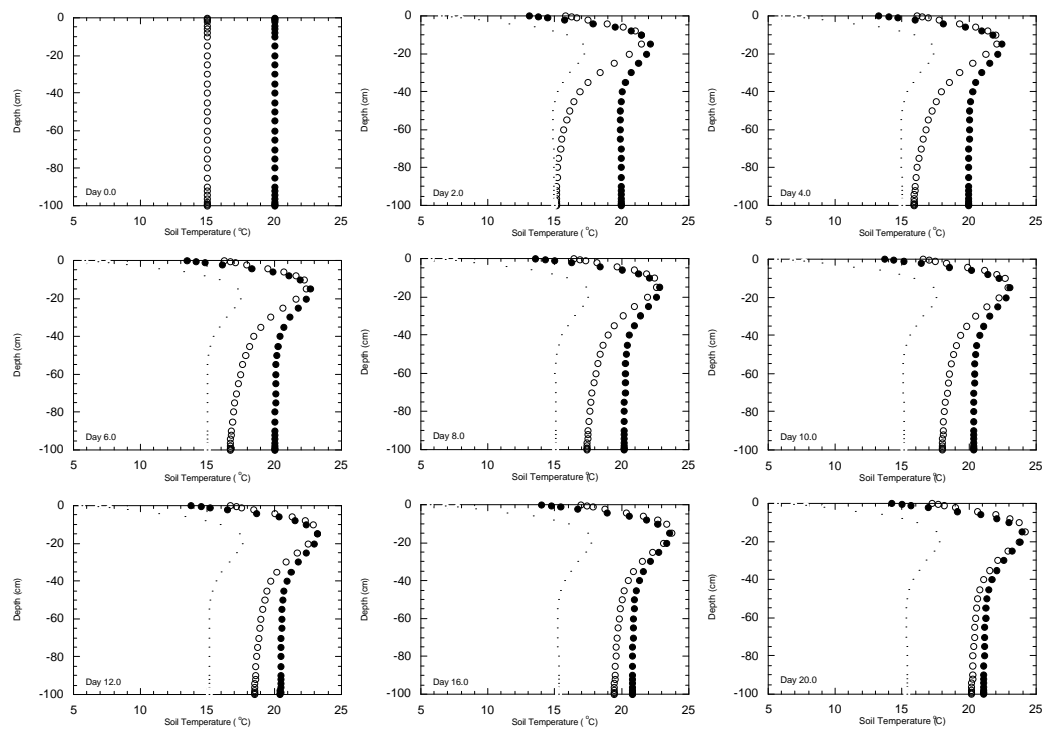


Figure 6.4: Comparison of soil temperature profile estimation using the continuous Dirichlet boundary condition for observations of the surface node (open circle) with the “true” soil temperature profile (solid circle) and the open loop soil temperature profile (open circle with dot).

likely from current technology. Temperature observations are for the surface node alone, as this is all that can be observed with thermal infra-red sensors.

The soil moisture and temperature profile estimation results are given in Figure 6.3 and Figure 6.4 respectively. In these figures, the “true” profiles are compared with the estimated profiles, as well as an “open loop” simulation. The open loop simulation is where no “observations” were used and the system was simply propagated from the initial conditions subject to the surface flux (Neumann) boundary conditions.

The estimated soil temperature profiles differ slightly for the different soil moisture observation depths, due to the difference in soil moisture profile estimation. This is a result of the dependence of soil thermal conductivity and heat capacity on the soil moisture, and the liquid mass flux. The estimated soil temperature profile plotted in Figure 6.4 is only for the 4 cm soil moisture observation depth, which is typical of the soil temperature results from other soil moisture observation depths.

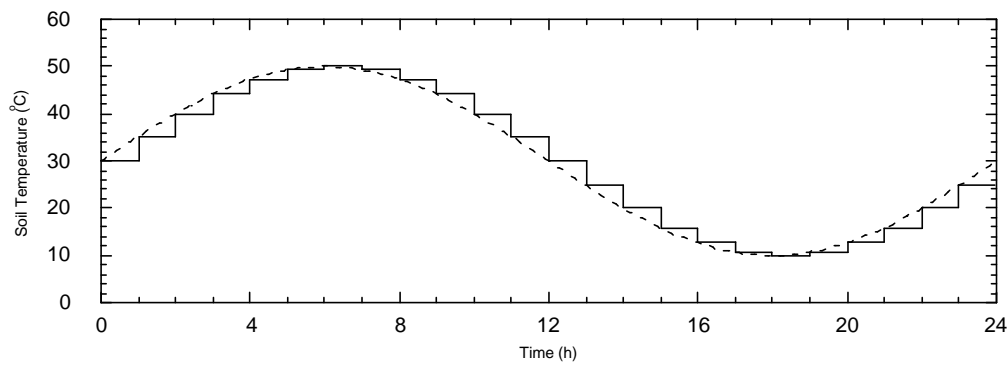


Figure 6.5: Illustration of the continuous Dirichlet boundary condition applied for estimation of the soil temperature profile. The dashed line is the “true” Dirichlet boundary condition while the solid line is the approximation to the Dirichlet boundary condition

The soil moisture content and soil temperature at the surface of the soil column change with time. In order to maintain the continuous Dirichlet boundary condition at the “true” value, it was necessary to update the near-surface values regularly. Therefore the near-surface values used for the continuous Dirichlet boundary condition were updated once every hour, with the “observed” value at the beginning of the one hour simulation period. Hence, the simulated soil temperature in Figure 6.4 always lagged behind the “true” soil temperature by one hour at the soil surface (see Figure 6.5).

The continuous Dirichlet boundary condition applies the “true” soil moisture and temperature values near the soil surface. Figure 6.3 and Figure 6.4 show how this boundary condition was slowly transferred from the near-surface to deeper depths by the model physics. Thus, starting from the soil surface, the profile estimation algorithm adjusted its estimate of the soil moisture and temperature profile towards the “true” soil moisture and temperature profile values, while the open loop showed no improvement. Since the system was drying and the poor initial guess was somewhat drier than that for the “true” profile, the open loop moisture profile continued to dry, diverging from the “true” profile.

The open loop soil temperature and moisture profiles responded differently to the soil moisture profile. As the system was subject to a diurnal soil heat flux, there was a diurnal soil temperature variation in the upper section of the soil profile, which continued to maintain its difference from the “true” soil temperature profile of approximately 5°C, except for very shallow depths. This difference near the soil surface was most likely due to the open loop soil moisture

profile becoming very much drier than the “true” soil moisture profile at the soil surface, which allowed greater temperature variations for the same soil heat flux, as a result of a reduced heat capacity of the soil.

When the Dirichlet boundary condition was applied over deeper depths, improvements in estimation of the soil moisture profile occurred more quickly. Soil moisture profile estimates coincided with the “true” soil moisture profile (ie. the “true” soil moisture profile was retrieved) after approximately 8 days for the Dirichlet boundary condition at the surface node. In comparison, the “true” soil moisture profile was retrieved after only approximately 5 days when updating the top 10 cm. Once the “true” soil moisture profile was retrieved, the model continued to track the “true” soil moisture profile. This was because there was no “model error” in these simulations, and the only reason for difference between the estimated, open loop, and “true” soil moisture profiles during early simulations, was the poor initial guess of the soil moisture profile.

Retrieval of the “true” soil temperature profile proceeded more slowly than for soil moisture, requiring more than 20 days. After 20 days, the estimated and “true” soil temperature profiles differed by less than 1°C at deeper depths.

6.4.2 UPDATING ONCE EVERY HOUR

As a first step towards more practically realistic one-dimensional soil moisture and temperature profile estimation, and to compare with Entekhabi *et al.* (1994), both the hard-update and Kalman-filter assimilation schemes were applied once every hour using surface “observations” with various observation depths. For the soil moisture equation, the observation depths were taken to be 0 (surface node), 1, 4 and 10 cm, while for the temperature equation the observation depth was taken as the surface node. The values that have been used for the surface “observations” were the simulation values from the “true” profiles for that time and depth.

This section looks at soil moisture and temperature profile estimation results from both zero moisture and heat flux at the base of the soil column (normal simulation) and gravity drainage and heat advection at the base of the soil column, for comparison with simulation results of Entekhabi *et al.* (1994). A

sensitivity analysis of soil moisture and temperature profile estimation to factors likely to influence the difference in Kalman-filter estimates of the soil moisture profile from those of Entekhabi *et al.* (1994) is also presented.

6.4.2.1 Normal Simulation

The normal simulation results include assimilation of near-surface observations using both the hard-updating and Kalman-filtering schemes. Hard-updating simulation results for soil temperature profile estimation showed little variation with soil moisture updating for different depths. Hence, the soil temperature profile estimation results are only given for hard-updating of the soil moisture profile with an observation depth of 4 cm. However, soil temperature profiles from Kalman-filtering are given for all soil moisture observation depths, This is because the Kalman-filter produced different soil temperature profile estimates for different soil moisture observation depths, as a result of its ability to make adjustments to the entire temperature profile, rather than just the surface node.

Hard-updating results are for the time step immediately prior to the update, whilst the profiles from the Kalman-filter assimilation scheme are the actual Kalman-filter update. This is the situation for all simulations presented in this thesis.

6.4.2.1.1 Hard-Updating

The hard-updating assimilation scheme performs an instantaneous replacement of the model estimate with the “true” soil moisture and temperature values over the observation depth once every hour. Thus, the only way in which extra soil moisture mass or heat energy could be added to or removed from the soil system was through the observations at the surface node(s). It can be seen from both Figure 6.6 (soil moisture) and Figure 6.7 (soil temperature) that if this information was only provided for the surface node, then there was no improvement in the profile estimates and the results were similar to those of the open loop. This was most likely because the model was driven by gradients, and the gradients at the nodes below the surface node over-rode the update, rapidly replacing the update value with the original value. However, when the time step

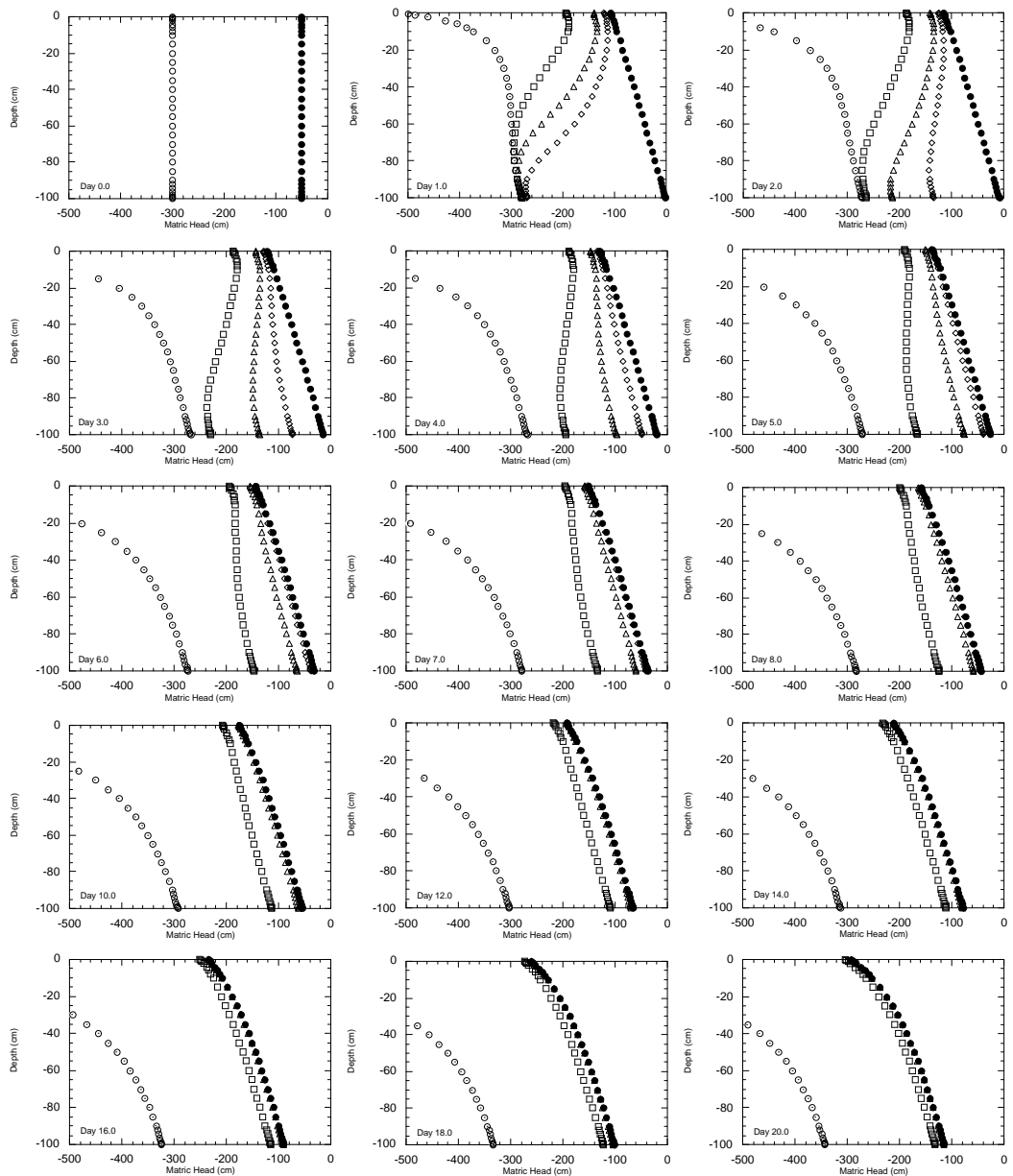


Figure 6.6: Comparison of soil moisture profile estimation using the hard-update assimilation scheme for observation depths of 0 (open circle), 1 (open square), 4 (open triangle) and 10 cm (open diamond) with the “true” soil moisture profile (solid circle) and the open loop soil moisture profile (open circle with dot).

size of the very first time step after the update was increased by three orders of magnitude, then some of the updating information at the surface node was passed to deeper depths.

The slight variation in the temperature profile from the open loop profile for the hard-update assimilation scheme was probably a result of the improvement in soil moisture profile estimates. This was because soil heat capacity and soil

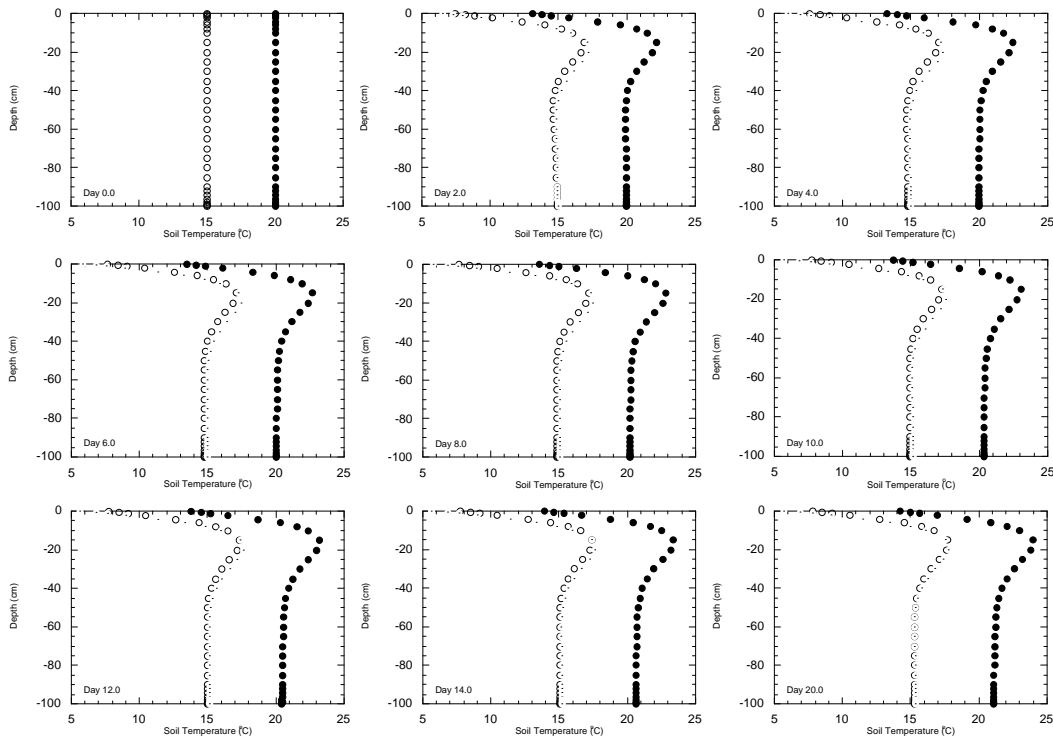


Figure 6.7: Comparison of soil temperature profile simulation using the hard-update assimilation scheme for observations of the surface node (open circle) with the “true” soil temperature profile (solid circle) and the open loop soil temperature profile (open circle with dot).

thermal conductivity are a function of soil moisture, and the soil temperature equation is a function of soil moisture content and the soil moisture flux.

Figure 6.6 shows that improvement in soil moisture profile estimation proceeded more quickly as the observation depth was increased, as was the case for the continuous Dirichlet boundary condition. However, the effect was much more pronounced here. This may be because the continuous Dirichlet boundary condition essentially controlled the rate of moisture flux near the soil surface, with the depth over which the continuous Dirichlet boundary condition was applied controlling the depth at which this flux was applied. Thus for deeper observation depths the flux was applied deeper within the soil column, resulting in a slightly reduced distance for propagation of this boundary condition into the soil profile, and hence a slightly faster improvement in soil moisture profile estimation. In hard-updating there was an update of the surface nodes for a given instant in time. Hence the “true” near-surface moisture flux was only applied for a short period of time, as this update information was redistributed to deeper depths relatively quickly, with the near-surface states and fluxes returning quickly to their original values. More importantly for the hard-update assimilation scheme, is that the

depth of update controlled the amount of soil moisture and heat energy that was added to the system for redistribution to deeper depths. It was this limited addition/subtraction of soil moisture mass and heat energy to the soil system in the hard-update assimilation scheme that made the effect of observation depth so pronounced.

Retrieval of the “true” soil moisture profile using hard-updating (Figure 6.6) required more than 20 days for observations over 1 cm, approximately 12 days for 4 cm and approximately 8 days for 10 cm. These retrieval times are significantly longer than for the continuous Dirichlet boundary condition of equivalent observation depth, especially for shallower observations, indicating that the extra soil moisture being added to the system through the update was playing a more prominent role than the effective Dirichlet boundary condition.

6.4.2.1.2 Kalman-Filtering

The Kalman-filter performed an instantaneous update of the entire profile once every hour, based on the relative magnitudes of the covariances of the observations and the model prediction. It could thus add or subtract soil moisture mass or heat energy from the system for more than just the near-surface nodes. However, the values assigned to the initial state covariance matrix, observation noise and system noise have a significant effect on the improvement in profile estimation. Hence for comparison with Entekhabi *et al.* (1994), their observation and model covariances, and system noise, should be replicated. Entekhabi *et al.* (1994) used an observation noise of 2% of the observed state (diagonal) and a system noise of 5% of the simulated system state (diagonal). However, the value assigned to the initial state covariances was not stated.

In this study, the initial state covariance matrix was 1000000 for the diagonal elements and zero for the off diagonal elements, representing a large uncertainty in the initial profile values and no correlation between nodes. The observation variances were 2% of the observed system state (matric head or soil temperature) for the diagonal elements and zero on the off diagonal elements. The system noise was 5% of the change in system states for each time step, for diagonal elements, compared with 5% of the actual system state value for

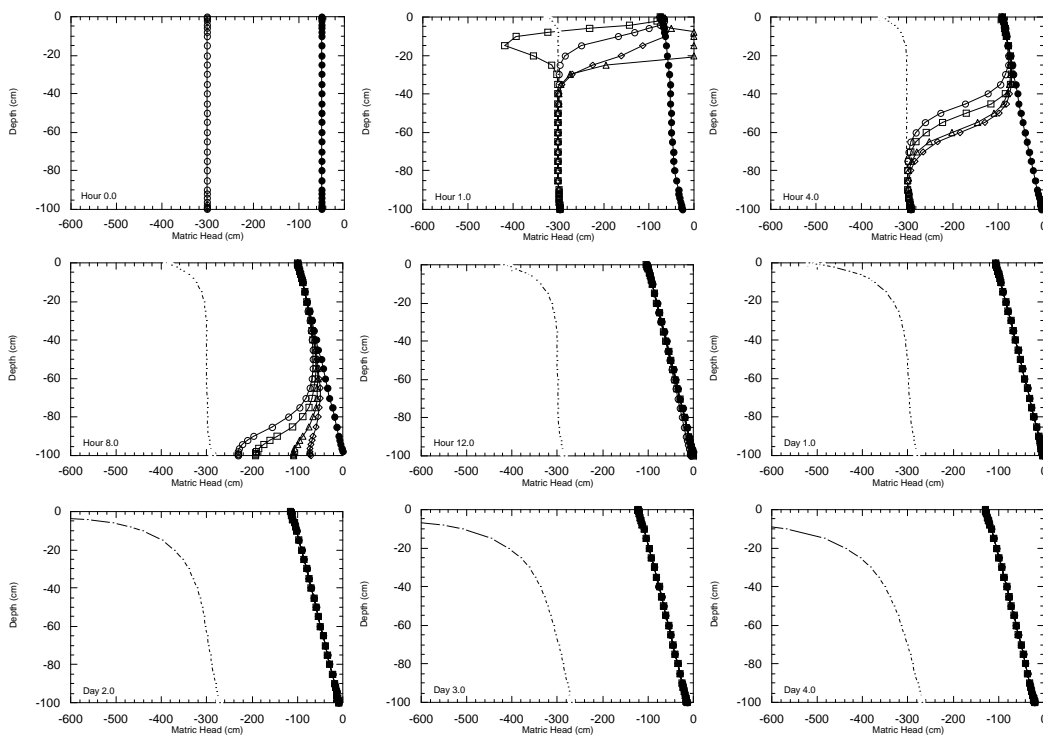


Figure 6.8: Comparison of soil moisture profile estimation using the Kalman-filter assimilation scheme for observation depths of 0 (open circle), 1 (open square), 4 (open triangle) and 10 cm (open diamond) with the “true” soil moisture profile (solid circle) and the open loop soil moisture profile (open circle with dot); initial state variances 1000000, observation variances 2% of observations and system noise 5% of change in states.

Entekhabi *et al.* (1994), and zero for the off diagonal elements. The reason for this was that adding 5% of the state to the diagonal elements of the system covariance matrix at each time step produced extremely large covariances, and was dependent on the number of time steps between observations.

Figure 6.8 shows that improvements in the soil moisture profile estimation proceeded more quickly as the observation depth was increased. However, there was not a great difference between the time taken to retrieve the “true” soil moisture profile for observations at the surface node and observations over a depth of 10 cm.

The updated moisture profile for the very first update at time 1 hour contained some artefacts, which were not present in later updates. These artefacts were a result of the initial state covariances and the poor initial guess. However, as the profile estimation algorithm proceeded, the state covariance matrix was “warmed up” and the difference between the forecast surface states and observations became less, so that a more uniform and systematic progression

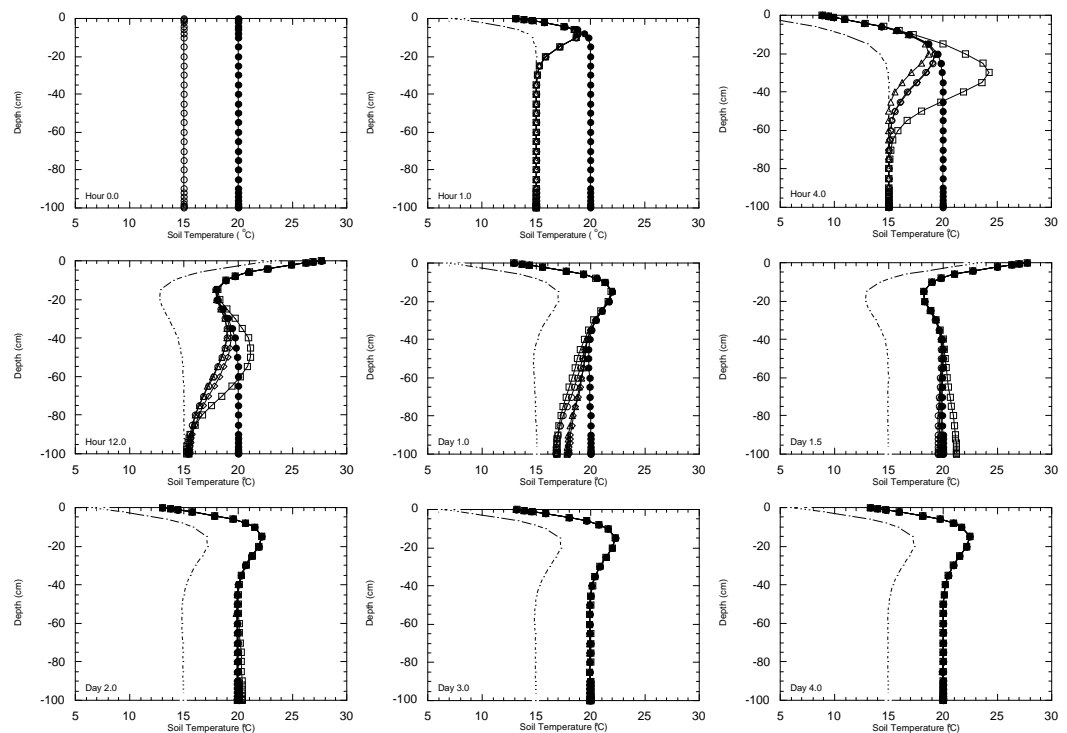


Figure 6.9: Comparison of soil temperature profile estimation using the Kalman-filter assimilation scheme for observations of the surface node (open symbols) with the “true” soil temperature profile (solid circle) and the open loop soil temperature profile (open circle with dot). Estimated soil temperature profiles correspond with soil moisture profile estimation for observations of 0 (open circle), 1 (open square), 4 (open triangle) and 10 cm (open diamond); initial state variances 1000000, observation variances 2% of observations and system noise 5% of change in states.

towards the “true” soil moisture profile was achieved. As the updating progressed, the Kalman-filter continued to make adjustments to the soil moisture profile at deeper depths until the “true” soil moisture profile was retrieved, at which stage the soil moisture profile estimation algorithm continued to track the “true” soil moisture profile.

Retrieval of the “true” soil moisture profile using the Kalman-filter assimilation scheme required only approximately 12 hours of updating each hour, independent of the observation depth. This is compared to 8 days for the hard-update assimilation scheme with observations over a depth of 10 cm, and no improvement for observations at the surface node. Retrieval of the “true” soil temperature profile using the Kalman-filter assimilation scheme (Figure 6.9) required approximately 2 days of updating, compared with no improvement for the hard-update assimilation scheme. These simulations show very convincingly that improvements in profile estimation using the Kalman-filter assimilation

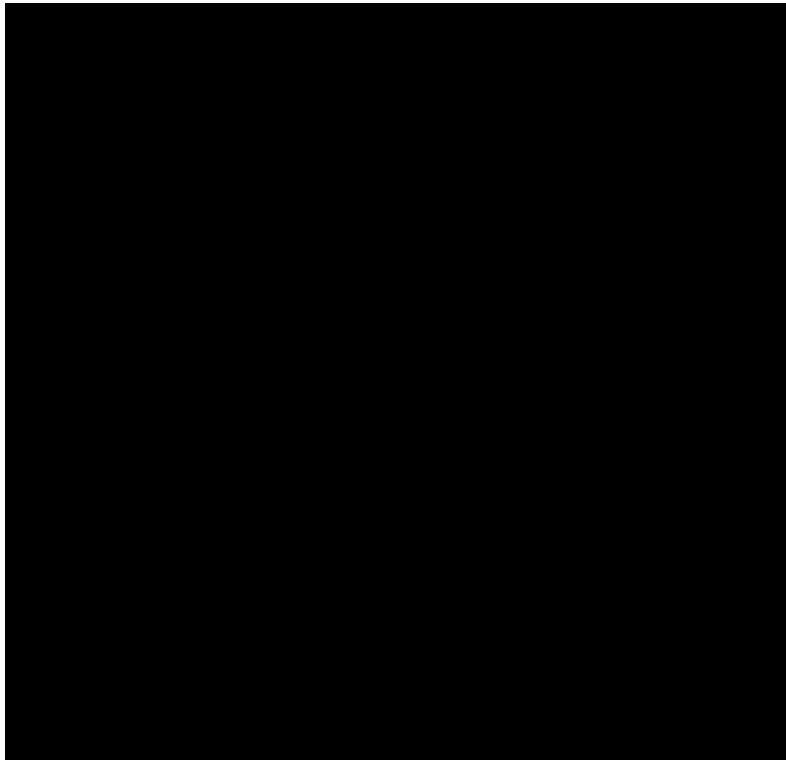


Figure 6.10: Entekhabi's comparison of soil moisture profile estimation using the Kalman-filter assimilation scheme (solid circles) with the "true" soil moisture profile (open circles) and open loop soil moisture profile (open triangle) (Entekhabi *et al.*, 1994)

scheme are a result of profile updating over depths greater than the observation depth.

Comparing the results in Figure 6.8 with those from Entekhabi *et al.* (1994) in Figure 6.10, it is obvious that the soil moisture profiles in their simulations dried much more quickly than in these simulations. Thus, it would appear that the boundary conditions applied to their model are somewhat different to those indicated. Either the evaporation rate indicated was too low, or there was a non-zero moisture flux boundary condition at the soil base. By undertaking simulations with various evaporation rates and boundary conditions, it became apparent that a gravity drainage boundary condition at the base of the soil column gave the closest comparison of soil moisture profiles with those of Entekhabi *et al.* (1994).

6.4.2.2 Gravity Drainage and Heat Advection Simulation

As the soil moisture profiles generated in Figure 6.8 were vastly different to those of Entekhabi *et al.* (1994), no conclusive comparison could be made with

their results. Thus, the hourly update simulations were repeated for gravity drainage and heat advection at the base of the soil column.

Comparison of “true” and open loop moisture profiles in Figure 6.6 (zero flux at base) with Figure 6.11 (gravity drainage) revealed a large difference. The soil moisture profiles with zero flux at the column base had an initial wetting up of lower depths in the profile, whilst the profiles from gravity drainage maintained the initial soil moisture content at depth. The effect of this was to increase the curvature of the matric head profile under the gravity drainage boundary condition.

The “true” soil moisture profile dried out much more quickly under the gravity drainage boundary condition, whilst the open loop profile dried out only slightly faster. This was due to the moisture control of the moisture flux at the soil column base, with the gravity drainage flux being greater for higher soil moisture contents, due to the greater hydraulic conductivity. Hence the “true” and open loop profiles did not diverge as quickly under the gravity drainage boundary condition. In addition, the moisture retention curve is exponential. Thus slight changes in volumetric soil moisture content had a corresponding large change in matric head at lower soil moisture contents, exacerbating the difference in “true” and open loop matric head profiles for the zero flux boundary condition. This would indicate that the use of a gravity drainage boundary condition should improve soil moisture profile estimation results, particularly through the moisture dependence on the gravity drainage, causing the “true” and open loop profiles to converge from the base. This also means that in practical applications, the underlying soil will change the characteristics of the soil moisture profile estimation process.

6.4.2.2.1 *Hard-Updating*

In both Figure 6.11 (soil moisture) and Figure 6.12 (soil temperature) it can be again seen that if hard-updates were made for the surface node alone, then there was no improvement in the profile estimation and the system continued in the same fashion as the open loop. As the soil moisture observation depth was increased, improvements in the soil moisture profile estimation were accomplished. The effect of increasing the observation depth on estimating the

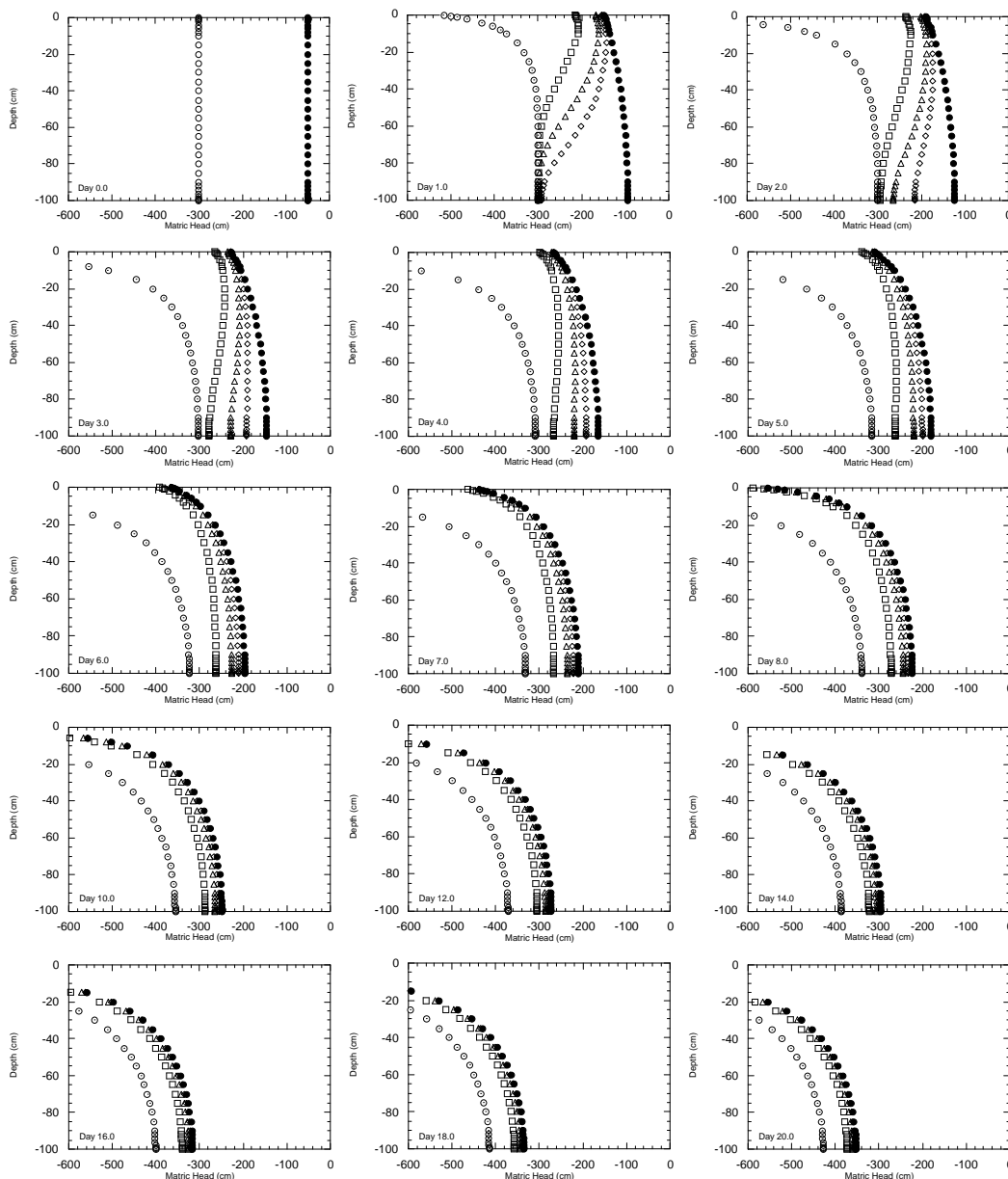


Figure 6.11: Comparison of soil moisture profile estimation using the hard-update assimilation scheme for observation depths of 0 (open circle), 1 (open square), 4 (open triangle) and 10 cm (open diamond) with the “true” soil moisture profile (solid circle) and the open loop soil moisture profile (open circle with dot). Gravity drainage boundary condition at base of soil column.

soil moisture profile was again much more pronounced than for the continuous Dirichlet boundary condition.

Retrieval of the “true” soil moisture profile using hard-updating required more than 20 days for observations over 1 cm, approximately 16 days for 4 cm and approximately 10 days for 10 cm. These times were slightly longer than for the zero flux boundary condition at the base of the soil column, which is counter intuitive. As time proceeds, the soil moisture profiles converged at the base of the

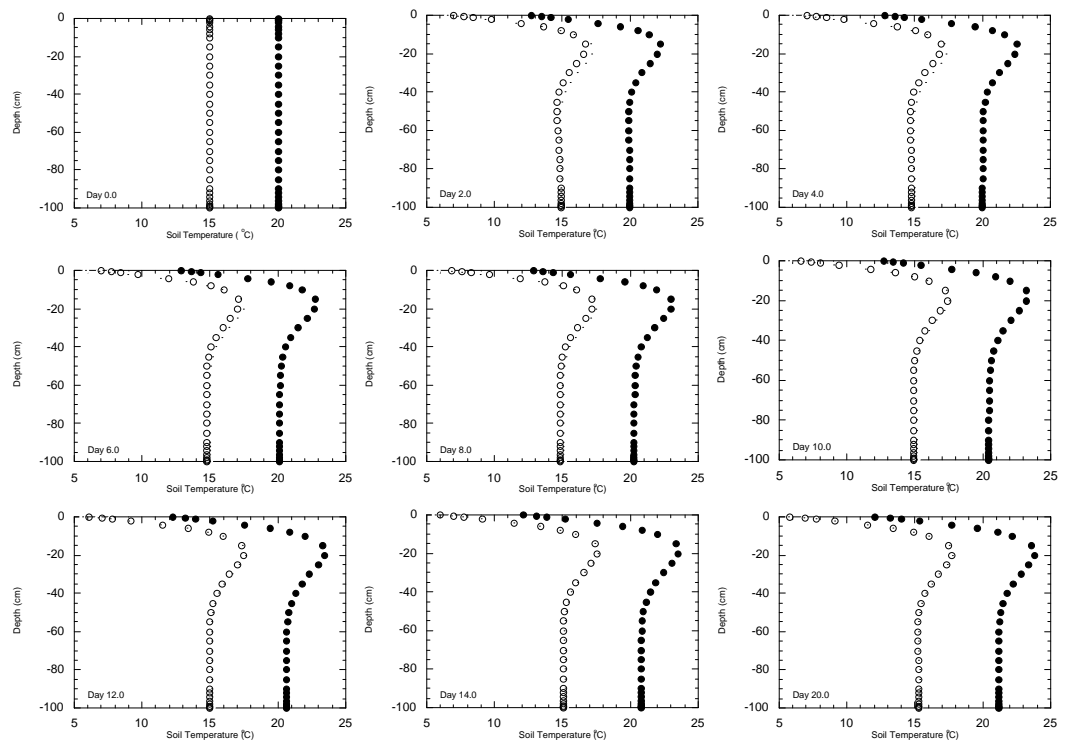


Figure 6.12: Comparison of soil temperature profile estimation using the hard-update assimilation scheme for observations of the surface node (open circle) with the “true” soil temperature profile (solid circle) and the open loop soil temperature profile (open circle with dot). Gravity drainage and advection boundary conditions at base of soil column.

soil column, as well as at the soil surface, due to the moisture control on the gravity drainage flux. This is the most notable difference between the simulations in Figure 6.6 and Figure 6.11

6.4.2.2.2 Kalman-Filtering

The soil moisture profile estimation results in Figure 6.13 for the Kalman-filter assimilation scheme have again shown that estimation of the “true” soil moisture profile proceeded slightly faster as the observation depth was increased. However, there was little time difference between the time required to retrieve the “true” soil moisture profile for observations at only the surface node and observations over a depth of 10 cm. The updated profiles in Figure 6.13 contain the same artefacts as were seen in Figure 6.8, with retrieval of the “true” soil moisture profile taking approximately 16 hours, independent of the observation depth. This is compared with 10 days for the hard-update assimilation scheme with observations over a depth of 10 cm. As for hard-updating, the time required to retrieve the “true” soil moisture profile using the Kalman-filter assimilation

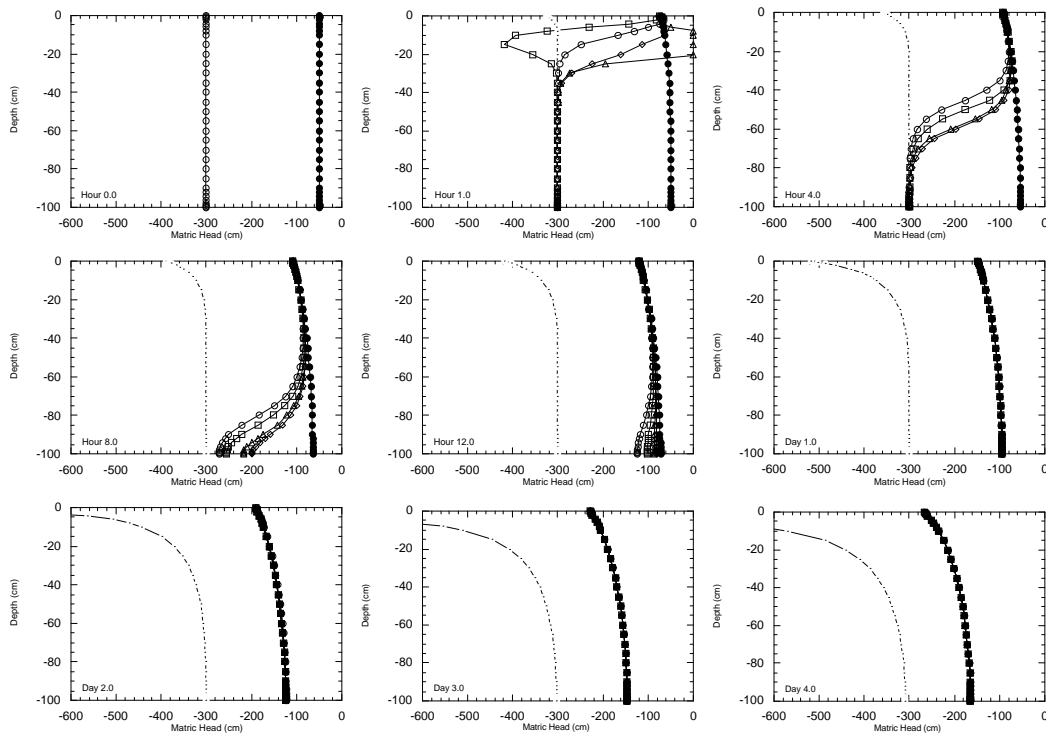


Figure 6.13: Comparison of soil moisture profile estimation using the Kalman-filter assimilation scheme for observation depths of 0 (open circle), 1 (open square), 4 (open triangle) and 10 cm (open diamond) with the “true” soil moisture profile (solid circle) and the open loop soil moisture profile (open circle). Gravity drainage boundary condition at base of soil column, initial state variances 1000000, observation variances 2% of observation and system noise 5% of change in states.

scheme for the gravity drainage was slightly longer than for the zero flux boundary condition.

Retrieval of the “true” soil temperature profile using the Kalman-filter assimilation scheme required approximately 2 days of updating (Figure 6.14), in comparison with no improvement in the estimates soil temperature profile for the hard-update assimilation scheme. The time required to retrieve the “true” soil temperature profile using the Kalman-filter for the gravity drainage and advection boundary conditions was approximately the same as for the zero flux boundary conditions.

The time taken for the soil moisture profile estimation algorithm to retrieve the “true” soil moisture profile using the Kalman-filter in Figure 6.13 was much shorter than that required by Entekhabi *et al.* (1994) in Figure 6.10, being approximately 16 hours as compared to approximately 4 days. Furthermore, it should also be noted that the profile estimation of Entekhabi *et al.* (1994) converged towards the “true” profile from the bottom. This is counter-intuitive, as

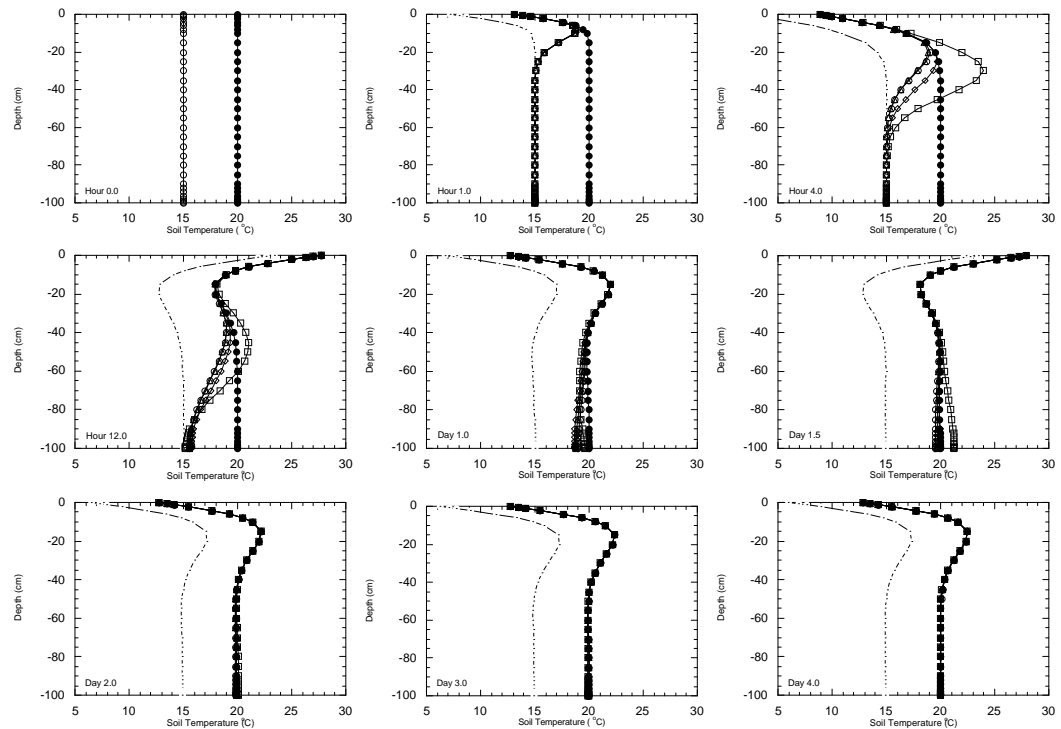


Figure 6.14: Comparison of estimated soil temperature profiles using the Kalman-filter assimilation scheme for observations of the surface node (open symbols) with the “true” soil temperature profile (solid circle) and the open loop soil temperature profile (open circle with dot). Estimated profiles correspond with soil moisture profile estimation for observation depths of 0 (open circle), 1 (open square), 4 (open triangle) and 10 (open diamond) cm. Gravity drainage and advection boundary conditions at base of soil column, initial state variances 1000000, observation variances 2% of observation and system noise 5% of change in states.

observations are made near the surface of the profile. Hence, it would be expected that improvements in the profile estimation would converge towards the “true” profile from the soil surface, as seen in the simulations so far in this thesis. However, for updating once every 5 days using extremely small initial state variances (Figure 6.37), improvements in soil moisture profile estimates converged towards the “true” soil moisture profile from the bottom of the soil column.

6.4.2.3 Sensitivity Analysis of Kalman-Filtering

There are three key factors that play a prominent role in the Kalman-filter assimilation scheme. Hence, differences in the soil moisture profile estimation as compared with Entekhabi *et al.* (1994) may be a result of differences in their specification. These factors are: (i) the initial state variances; (ii) the system noise; and (iii) the observation noise. As the initial state variances used by Entekhabi *et al.* (1994) were not stated, the initial state variances are likely to be different.

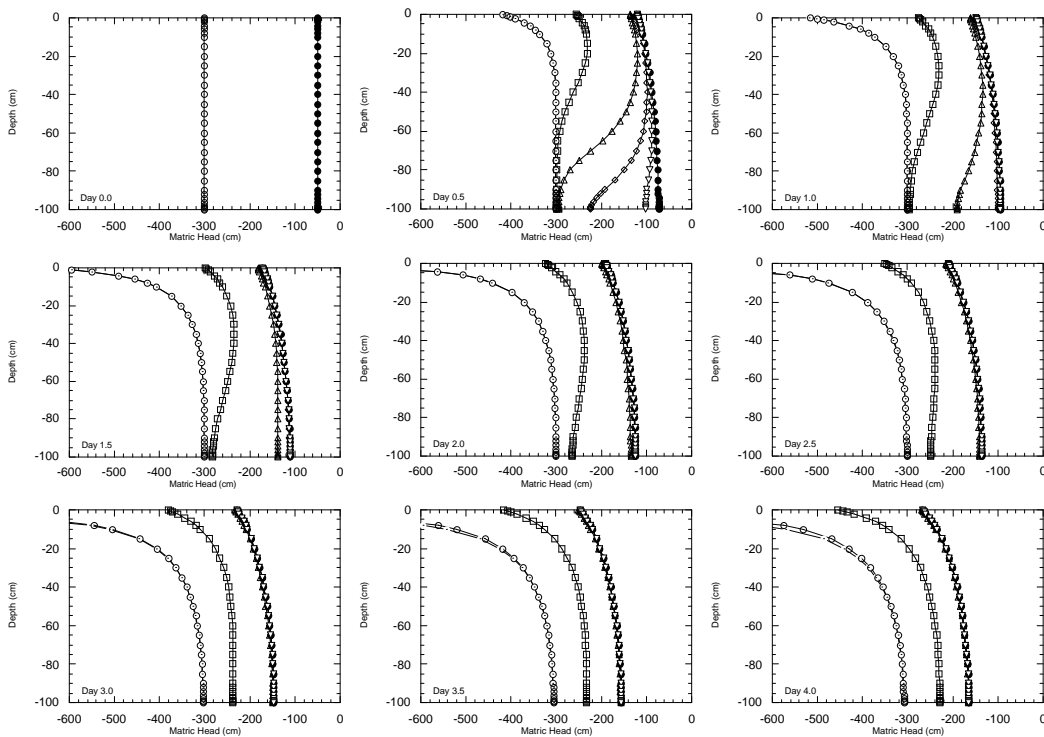


Figure 6.15: Comparison of soil moisture profile estimation using the Kalman-filter assimilation scheme for an observation depth of 1 cm with initial variances of 0 (open circle), 1 (open square), 100 (open upward triangle), 10000 (open diamond) and 1000000 (open downward triangle) with the “true” soil moisture profile (solid circle) and the open loop soil moisture profile (open circle with dot). Gravity drainage boundary condition at base of soil column, system noise of 5% of the change in system state during the time step and observation noise of 2% of the observation.

Also, application of the system noise by Entekhabi *et al.* (1994) is unclear, meaning that the system noise used was not identical. Furthermore, the observations used by Entekhabi *et al.* (1994) for soil moisture profile estimation were the simulated brightness and thermal infra-red temperatures, and the observations used in this study were the system states (matric head and soil temperature) for a given observation depth. Thus, the observation noise, being a proportion of the observed state value, was different for these two situations. To identify the effect of these three factors on estimation of the soil moisture profile using the Kalman-filter, a sensitivity analysis of the initial state variances, observation noise and system noise was performed, for a moisture observation depth of 1 cm. The effect of model discretisation was also assessed.

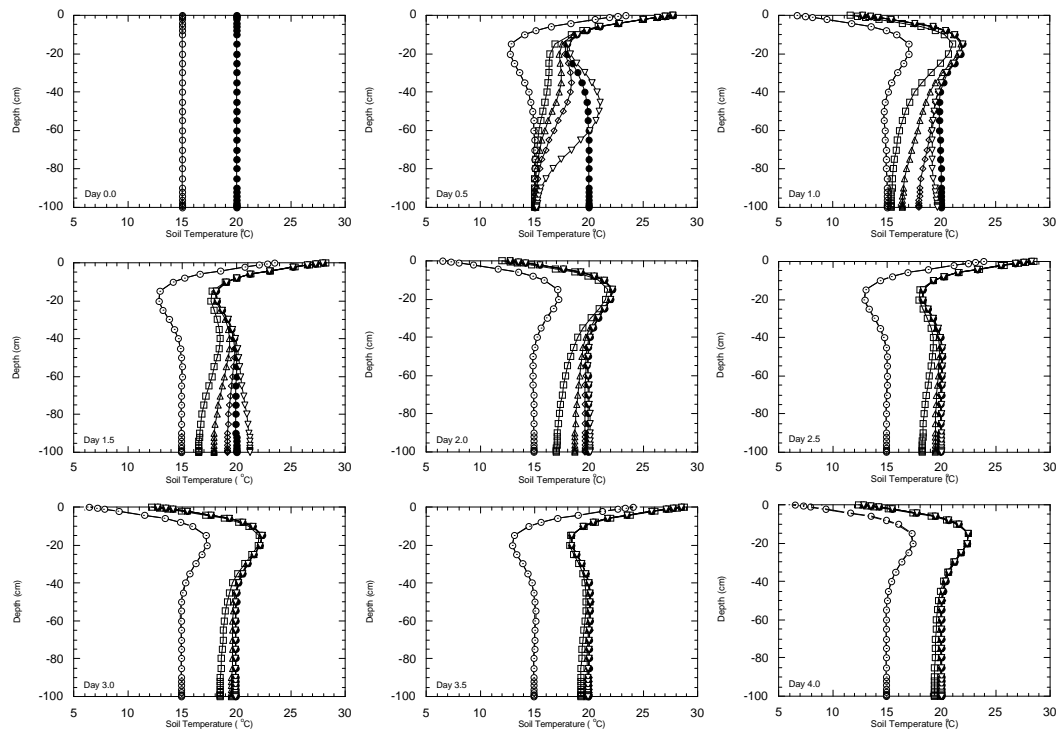


Figure 6.16: Comparison of soil temperature profile estimation using the Kalman-filter assimilation scheme for observations of the surface node with initial variances of 0 (open circle), 1 (open square), 100 (open upward triangle), 10000 (open diamond) and 1000000 (open downward triangle) with the “true” soil temperature profile (solid circle) and the open loop soil temperature profile (open circle with dot). Gravity drainage and advection boundary conditions at base of soil column, system noise of 5% of the change in system state during the time step and observation noise of 2% of the observation.

6.4.2.3.1 Sensitivity to Initial State Variances

The initial state variances specify one’s confidence in the initial state values. Giving these variances a large value signifies little confidence in the initial state values, allowing the Kalman-filter to make strong updates, providing the observation variances are comparatively low. The value assigned to the initial state variances will therefore have a major influence on the ability of the Kalman-filter to make strong updates. To identify how important this was, simulations were performed for initial state variances of 0, 1, 100, 10000 and 1000000, with a system noise of 5% of the change in system state during the time step and observation noise of 2% of the observed state value. These simulations are given in Figure 6.15 for soil moisture and Figure 6.16 for soil temperature.

Both Figure 6.15 and Figure 6.16 confirm that updating proceeds more cautiously as the initial state variances are reduced. However, the estimated soil moisture profile still proceeded towards the “true” soil moisture profile from the

surface down, unlike the results given by Entekhabi *et al.* (1994). Retrieval of the “true” soil moisture profile required approximately 16 hours, 1 day, 2 days and more than 4 days, while retrieval of the “true” soil temperature profile required approximately 2 days, 2 days, 2.5 days and 4 days for initial state variances of 1000000, 10000, 100 and 1 respectively. There was no improvement in profile estimation for an initial state variance of zero. This was expected, as an initial state variance of zero suggests that the initial states were known exactly for the entire soil profile. Hence, information contained in the observations was ignored as it was considered more likely to be in error than the model estimates of the system states. An initial state variance of 1 still allowed improvement in the profile estimates, even though it represented a very low uncertainty in the initial profile states, albeit at a much slower rate. Retrieval of the “true” profiles was still achieved for the initial state variance of 1, as this small variance signified to the filter that there was some uncertainty in the model states, and that some knowledge may be gained from the observations, provided that the uncertainty in the observations was not too great.

6.4.2.3.2 Sensitivity to System Noise

In addition to the initial state variances, the system noise has a major influence on the magnitude of the system state covariances, through the covariance propagation equation. When model updates are performed by the Kalman-filter, the system state covariances are reduced to account for the extra knowledge gained from the observations, based on Bayes theory. Thus, if there is no system noise term, the system state covariances can eventually go to zero. If the model was perfect, then this would be satisfactory. However, the majority of models are far from perfect, especially when linearisation is required. Thus, the system noise term is included to account for the uncertainty in covariance propagation caused by errors in state propagation. This has the effect of increasing the system state covariances during the inter-observation periods.

To quantitatively identify the sensitivity of improvements in soil moisture and temperature profile estimates to the system noise, simulations were performed for a system noise of 0, 2, 5, 10 and 20% of the change in system state during each forecast time step, with an observation noise of 2% of the observed state and

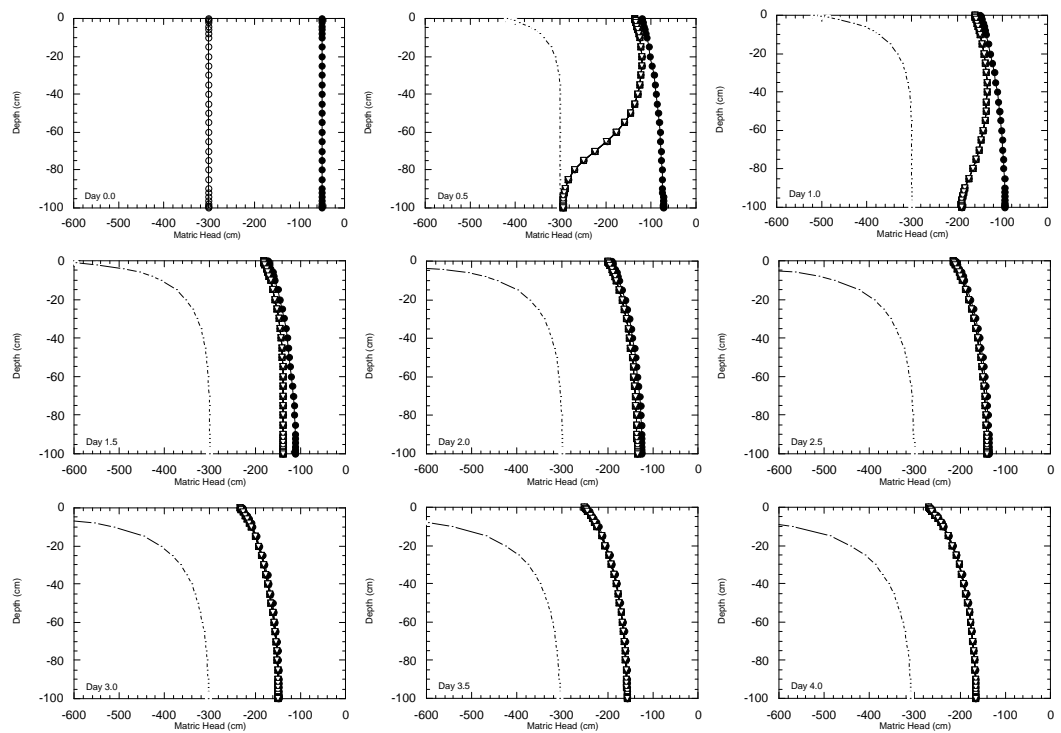


Figure 6.17: Comparison of soil moisture profile estimation using the Kalman-filter assimilation scheme for an observation depth of 1 cm having a model noise of 0 (open circle), 2 (open square), 5 (open upward triangle), 10 (open diamond) and 20 % (open downward triangle) of the change in system state during the time step with the “true” soil moisture profile (solid circle) and the open loop soil moisture profile (open circle with dot). Gravity drainage boundary condition at base of soil column, observation noise of 2% of the observation and initial covariances of 100.

an initial state variance of 100. An initial state variance of 100 was used for several reasons: (i) it allowed for slower convergence of the estimated profile towards the “true” profile, which was more representative of the profile estimation given by Entekhabi *et al.* (1994); and (ii) the effects from the different values of system noise were more apparent for a lower initial state variance. These simulations are given in Figure 6.17 for soil moisture and Figure 6.18 for soil temperature.

Both Figure 6.17 and Figure 6.18 have shown that changing the system noise had a minimal effect on the improvement in soil moisture and temperature profile estimation for this particular situation, with no noticeable differences over the range of system noise used. However, this may not be the case for a different form of system noise, as only relatively small changes were made in the system states for each time step, resulting in relatively low levels of system noise for each of the cases simulated. Different forms of system noise could be: (i) a percentage of the maximum change in state over the entire profile for the time step; or (ii) a

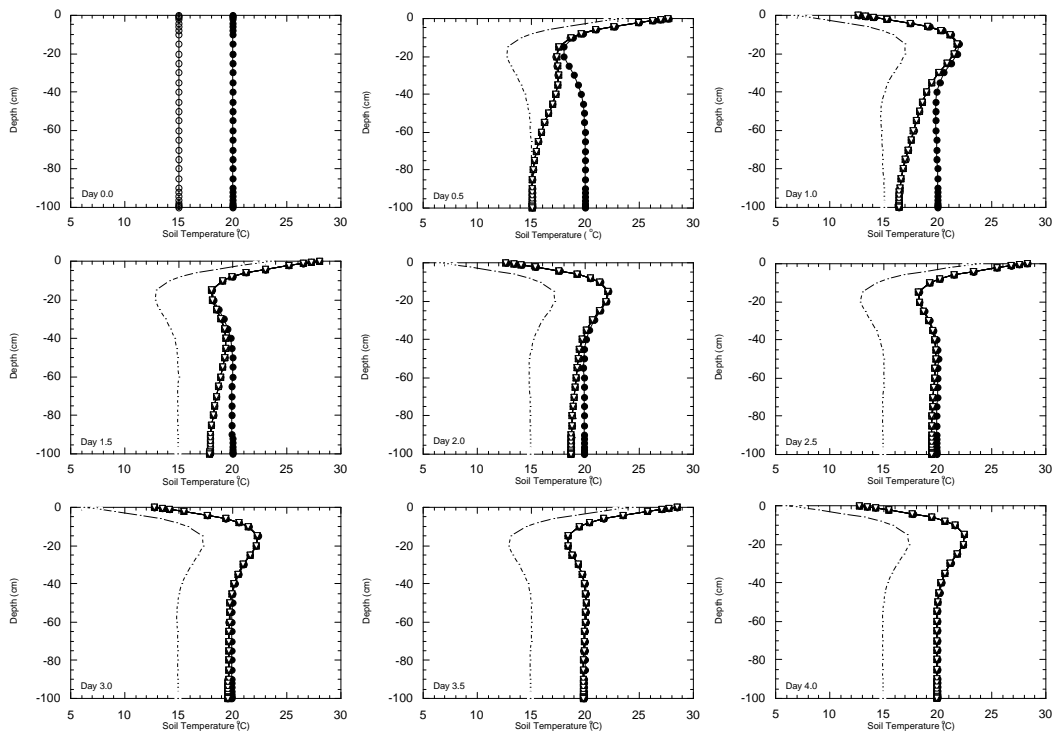


Figure 6.18: Comparison of soil temperature profile estimation using the Kalman-filter assimilation scheme for observations of the surface node having a model noise of 0 (open circle), 2 (open square), 5 (open upward triangle), 10 (open diamond) and 20% (open downward triangle) of the change in system state during the time step with the “true” soil temperature profile (solid circle) and the open loop soil temperature profile (open circle with dot). Gravity drainage and advection boundary conditions at base of soil column, observation noise of 2% of the observation and initial variances of 100.

percentage of the actual state value, normalised to account for time step size. In this way, the system state covariances would not be affected by the number of time steps taken between observations.

6.4.2.3.3 Sensitivity to Observation Noise

Apart from system state covariances, the rate of improvement in profile estimation could be influenced by the observation noise. The reason for this is that Kalman-filter updates are made based on the relative magnitudes of the system state and observation covariances. Thus, if the system state observation covariances are large relative to the observation covariances, the Kalman-filter places its faith in the observations over the model states, making large adjustments to the model profiles. If on the other hand the observation covariances are large in comparison to the modelled system state covariances, the Kalman-filter places its faith in the model states over the observations, making only minor adjustments to the model profiles. To quantitatively identify the

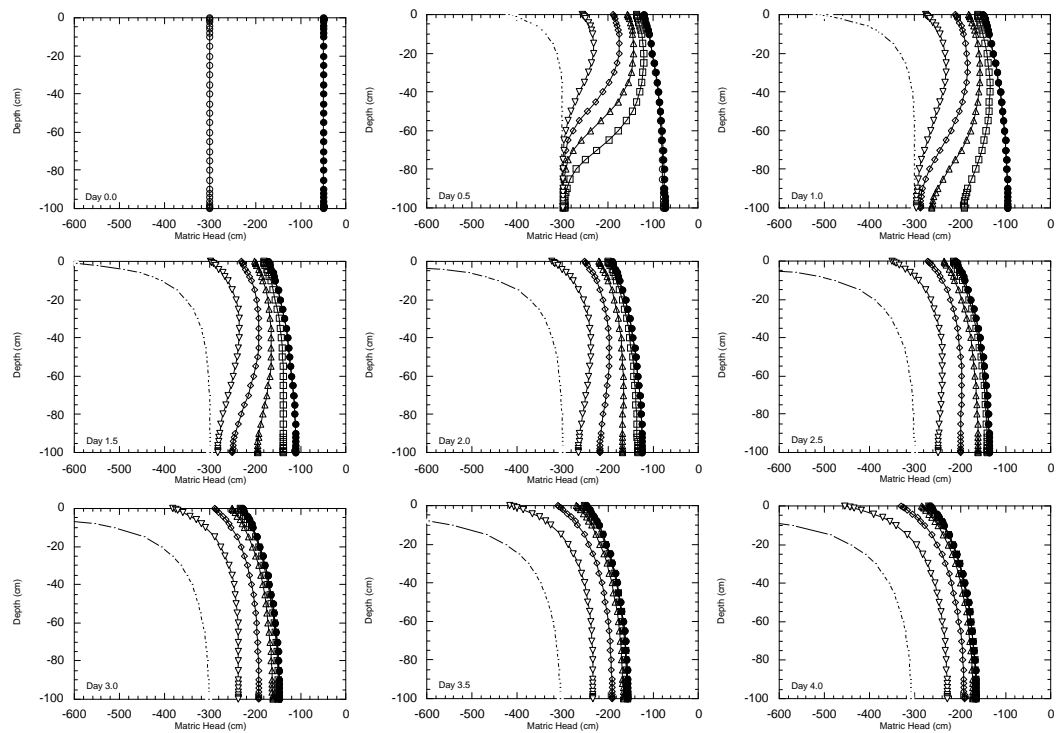


Figure 6.19: Comparison of soil moisture profile estimation using the Kalman-filter assimilation scheme for an observation depth of 1 cm with an observation noise of 0 (open circle), 2 (open square), 5 (open upward triangle), 10 (open diamond) and 20% (open downward triangle) of the observation with the “true” soil moisture profile (solid circle) and the open loop soil moisture profile (open circle with dot). Gravity drainage boundary condition at base of soil column, system noise of 5% of the change in system state during the time step and initial variances of 100.

sensitivity of improvements in profile estimation to the observation covariances, simulations were performed for an observation noise of 0, 2, 5, 10 and 20% of the observed state, with an initial state variance of 100 and system noise of 5% of the change in system state during the time step. These simulations are given in Figure 6.19 for soil moisture and Figure 6.20 for soil temperature.

Both Figure 6.19 and Figure 6.20 have shown that changing the observation noise had a strong influence on improvements in the estimation of soil moisture and temperature profiles, with the rate of improvement in profile estimation becoming slower as the observation noise was increased. This agrees with expectations. The rate of improvement in profile soil moisture estimates occurred much more quickly for “perfect” observations than for even a very low level of observation noise (2%), with retrieval of the “true” soil moisture profile requiring approximately 12 hours of updating as compared to 2.5 days. This was not the case for estimation of the soil temperature profile, with retrieval of the “true” soil temperature profile requiring approximately 2.5 days of updating for

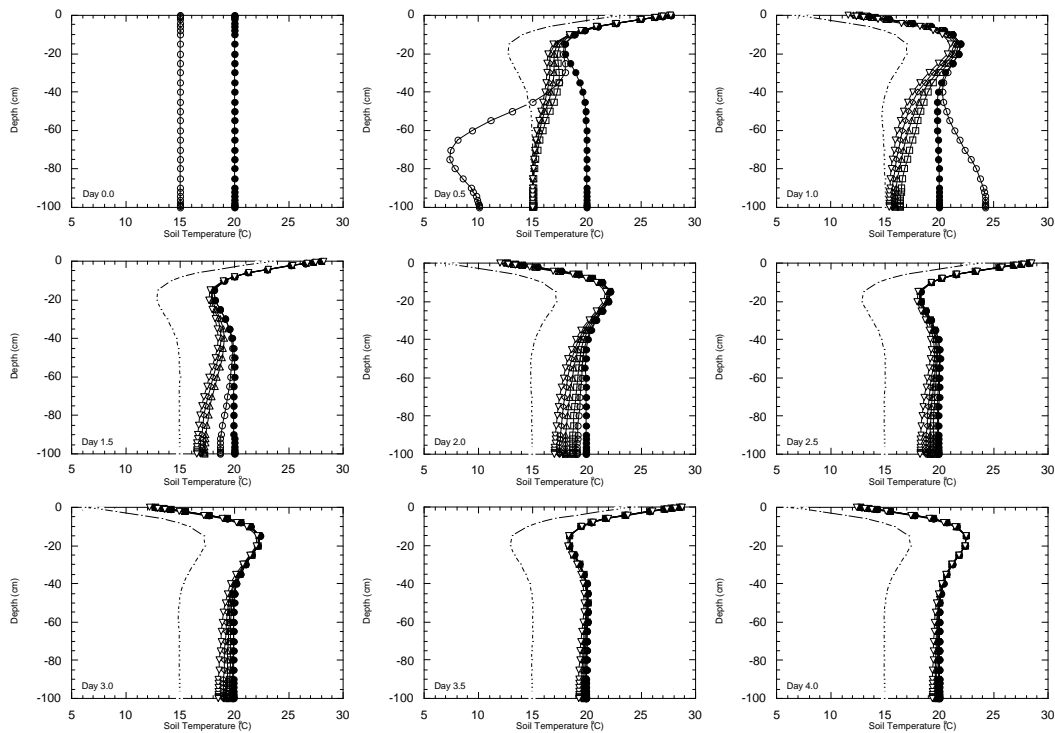


Figure 6.20: Comparison of soil temperature profile estimation using the Kalman-filter assimilation scheme for observations of the surface node with an observation noise of 0 (open circle), 2 (open square), 5 (open upward triangle), 10 (open diamond) and 20% (open downward triangle) of observation with the “true” soil temperature profile (solid circle) and the open loop soil temperature profile (open circle with dot). Gravity drainage and advection boundary conditions at base of soil column, system noise of 5% of the change in system state during the time step and initial variances of 100.

both situations, and 3.5 days for higher levels of observation noise. However, temperature profile updating with “perfect” observations caused some erratic updating at deeper depths, whilst the “noisy” observations proceeded cautiously in a monotonic manner towards the “true” profile.

Using a very low initial state variance of 100, system noise of 5% of change in states during the time step and observation variance of 5% of observations, resulted in a soil moisture retrieval time that was similar to that of Entekhabi *et al.* (1994). However, the way in which the estimated soil moisture profile approached the “true” soil moisture profile was not consistent with their results.

6.4.2.3.4 Sensitivity to Model Discretisation

Another factor that could possibly have an influence on the Kalman-filter update is the number of nodes in the observation depth. Therefore, for soil

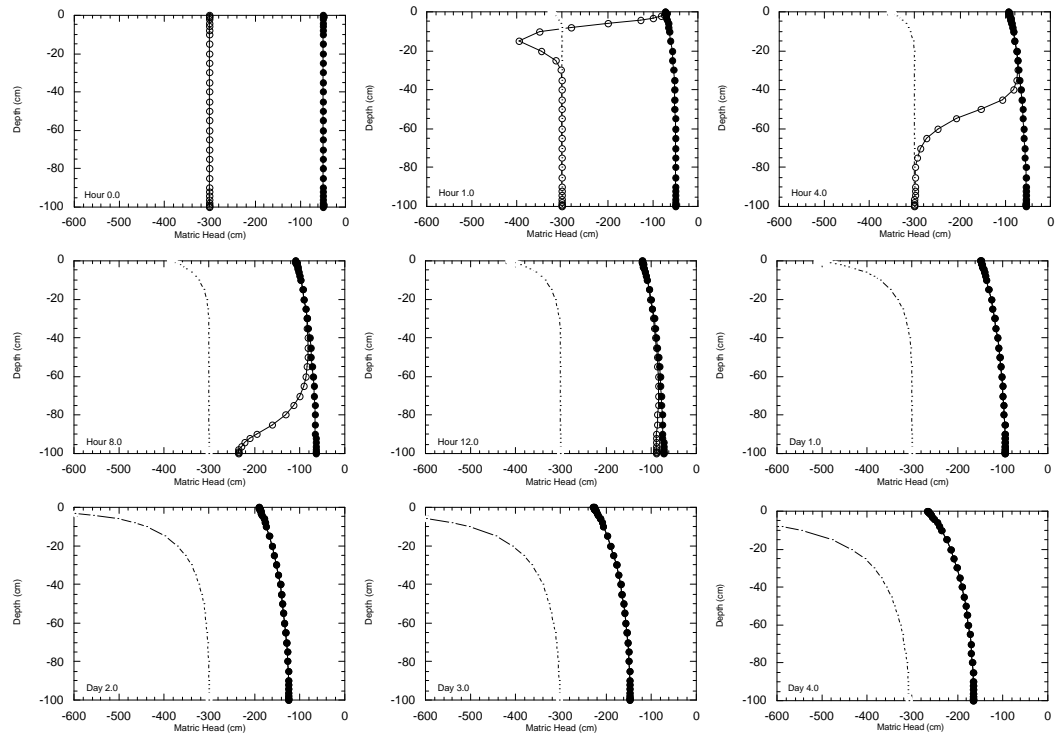


Figure 6.21: Comparison of soil moisture profile estimation using the Kalman-filter assimilation scheme for an observation depth of 1 cm (open circle) with the “true” soil moisture profile (solid circle) and the open loop soil moisture profile (open circle with dot) for an increased number of near-surface nodes. Gravity drainage boundary condition at base of soil column, system noise of 5% of the change in system state during the time step, observation noise of 2% of the observation and initial state variances of 1000000.

moisture updating over a depth of 1 cm, the number of nodes in the top 1 cm of the soil profile was increased from 3 to 10. The results from this simulation are given in Figure 6.21 for soil moisture and Figure 6.22 for soil temperature.

Comparison of Figure 6.21 and Figure 6.22 with Figure 6.13 and Figure 6.14 indicate that increasing the number of nodes within the observation depth had a minimal effect on estimation of the “true” soil moisture and temperature profiles. These simulations indicate a low sensitivity of the rate of improvement in soil moisture and temperature profile estimation and the shape of these profiles to the number of nodes in the observation depth.

6.4.3 UPDATING ONCE EVERY DAY

An observation frequency of once every hour is unrealistic for any practical application of soil moisture profile estimation from remotely sensed near-surface soil moisture observations. At best, we may expect a repeat coverage of once every day. However, the results from updating once every hour are

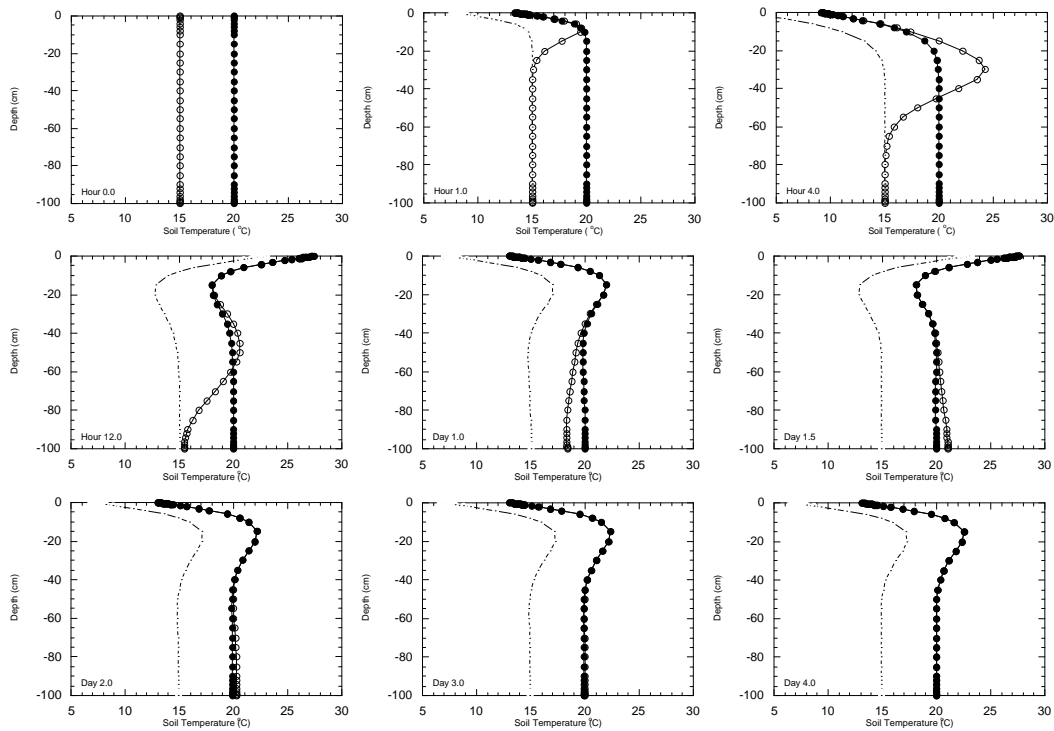


Figure 6.22: Comparison of soil temperature profile estimation using the Kalman-filter assimilation scheme for observations of the surface node (open circle) with the “true” soil temperature profile (solid circle) and the open loop soil temperature profile (open circle with dot) for an increased number of near-surface nodes. Gravity drainage and advection boundary conditions at base of soil column, system noise of 5% of the change in system state during the time step, observation noise of 2% of the observation and initial state variances of 1000000.

applicable to soil moisture profile estimation from a single soil moisture probe that is monitoring near-surface soil moisture content at a weather station.

To assess the viability of estimating soil moisture and temperature profiles from daily observations, both the hard-update and Kalman-filter assimilation schemes were applied for near-surface observations once every day. This study was undertaken in the same manner as for updating once every hour, with the boundary condition at the base of the soil column being zero moisture and heat flux. This is the boundary condition used for all of the simulations that follow in this chapter.

6.4.3.1 *Hard-Updating*

The soil moisture and soil temperature profile estimation results using the hard update assimilation scheme for observations once every day are given in Figure 6.23 for soil moisture and Figure 6.24 for soil temperature. The results in Figure 6.23 indicate once more the benefit of an increased depth knowledge with

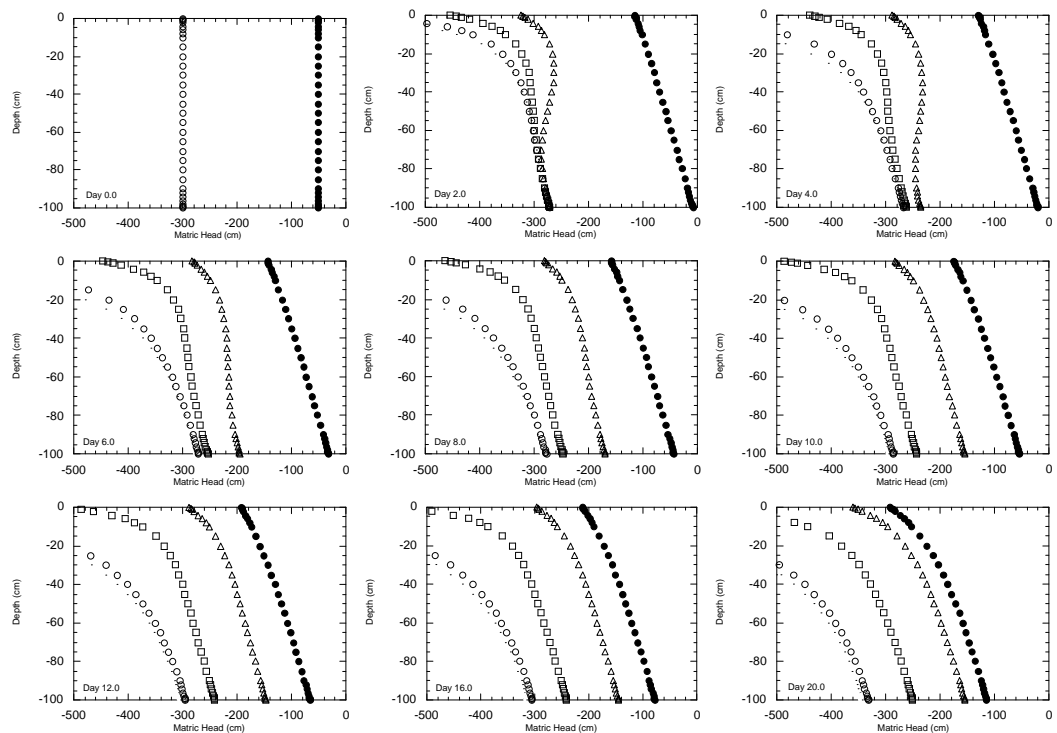


Figure 6.23: Comparison of soil moisture profile estimation using the hard-update assimilation scheme over depths of 1 (open circle), 4 (open square) and 10 cm (open triangle) with the “true” soil moisture profile (solid circle) and the open loop soil moisture profile (open circle with dot).

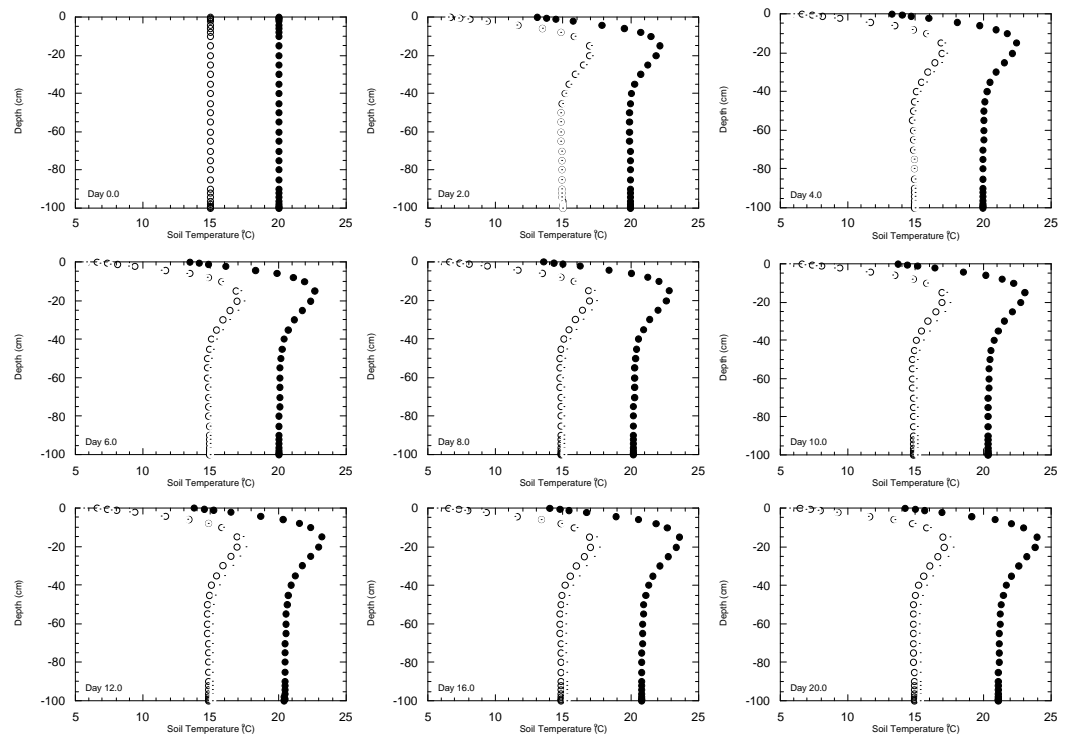


Figure 6.24: Comparison of soil temperature profile estimation using the hard-update assimilation scheme for observations of the surface node (open circle) with the “true” soil temperature profile (solid circle) and the open loop soil temperature profile (open circle with dot).

hard-updating. An observation depth of 10 cm facilitated improvement in the soil moisture profile estimation much more rapidly than for 4 cm, whilst an observation depth of 1 cm resulted in essentially no improvement after 20 days. This was due to the soil moisture mass balance problem discussed in the previous section.

An observation depth of 1 cm is representative of what can be achieved from most current remote sensing systems. Hence, it is obvious that a means of allowing extra soil moisture mass to be added to or subtracted from the system (as the case may be) must be identified, in order for the hard-update assimilation scheme to be effective for realistic observation depths and observation intervals. Figure 6.24 showed once more the failure to make improvements to the soil temperature profile estimation from an instantaneous hard-update for only the surface node. Thus for soil temperature profiles to be estimated correctly under the hard-update assimilation scheme, a means for allowing extra heat energy to be added to or subtracted from the system was also required.

6.4.3.2 Hard-Updating and Dirichlet Boundary Condition

The most obvious solution to the soil moisture mass and heat energy balance problem with the hard-update assimilation scheme was to perform the hard-update and then hold the update values fixed for some period of time. Providing it is not raining, both soil moisture and temperature values do not change much over a period of 1 hour. Thus, the hard-update assimilation scheme was applied with a Dirichlet boundary condition for a period of 1 hour. The results from this simulation are given in Figure 6.25 for soil moisture and Figure 6.26 for soil temperature. This simulation differs from the continuous Dirichlet boundary condition simulations in section 6.4.1 in that the Dirichlet boundary condition was only applied for 1 hour out of every 24 hour period.

Figure 6.25 shows that use of the Dirichlet boundary condition improves estimation of the soil moisture profile, and that improvements in soil moisture profile estimation still occurred more quickly for deeper observation depths. Improvements in soil moisture profile estimation using the 1 cm observation depth were quicker than improvements in soil moisture profile estimation using the 4 cm observation depth without the Dirichlet boundary condition.

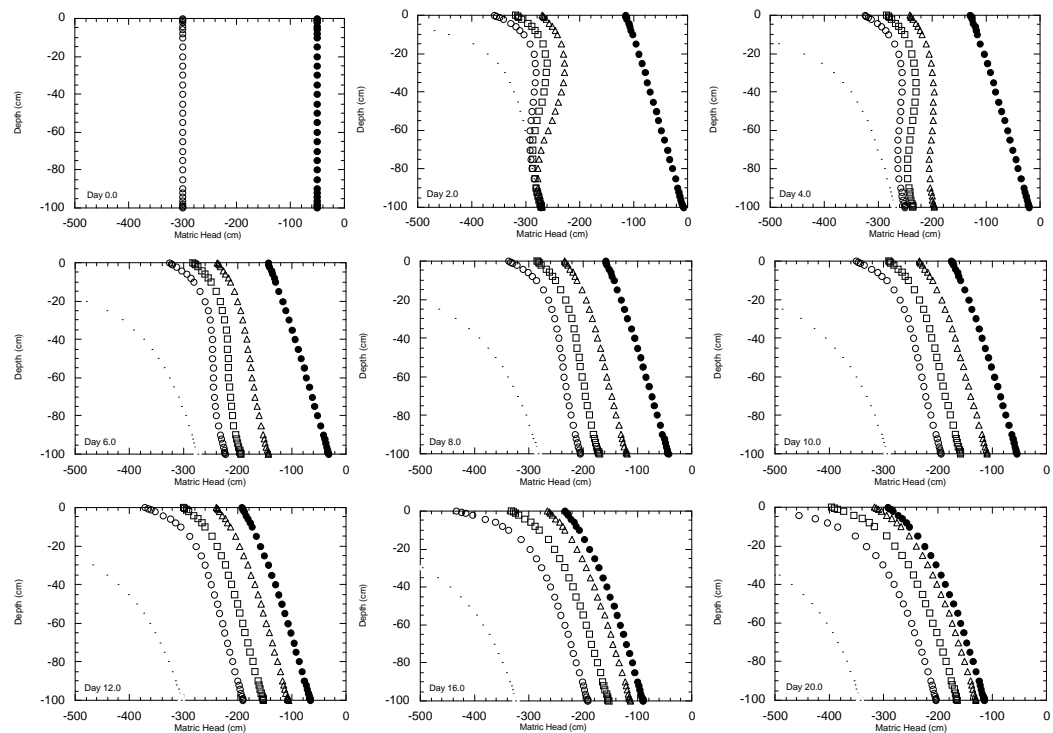


Figure 6.25: Comparison of soil moisture profile estimation using the hard-update assimilation scheme with a Dirichlet boundary condition for 1 hour over observation depths of 1 (open circle), 4 (open square) and 10 cm (open triangle) with the “true” soil moisture profile (solid circle) and the open loop soil moisture profile (open circle with dot).

Improvements in soil moisture profile estimation for the 4 cm observation depth were approximately equivalent to improvements in soil moisture profile estimation for the 10 cm observation depth without the Dirichlet boundary condition. Furthermore, improvements in estimation of the soil moisture profile for the 4 cm observation depth were approximately twice as fast as for the 1 cm observation depth, and the 10 cm observation depth was approximately twice as fast again.

By using the Dirichlet boundary condition for a period of 1 hour after the update, improvements in estimation of the soil moisture profile were achieved for all observation depths. However, retrieval of the “true” soil moisture profile did not occur within 20 days. Likewise, improvements in estimation of the soil temperature profile were achieved from observation of the soil skin temperature, but retrieval of the “true” soil temperature profile did not occur within the 20 days. Hard-updating once every day, even with a Dirichlet boundary condition for 1 hour period, yielded significantly slower retrieval of the “true” soil moisture profile than an instantaneous hard-update once every hour (8 days as compared to

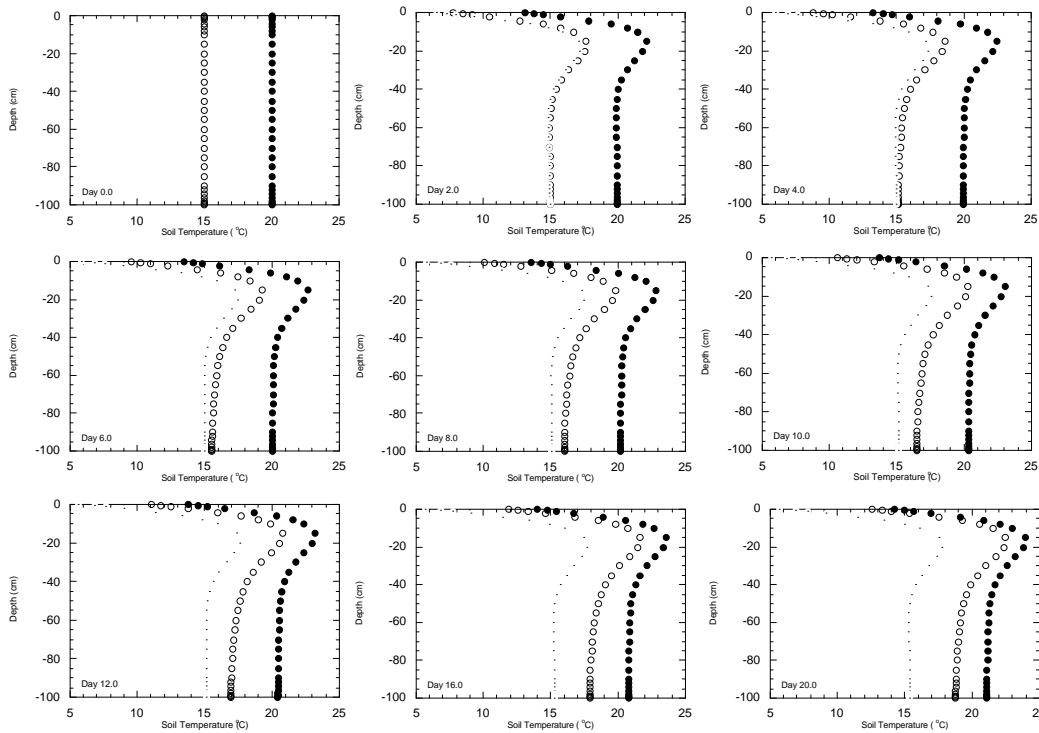


Figure 6.26: Comparison of soil temperature profile estimation using the hard-update assimilation scheme with a Dirichlet boundary condition for 1 hour at the surface node (open circle) with the “true” soil temperature profile (solid circle) and the open loop soil temperature profile (open circle with dot).

more than 20 days for the 10 cm observation depth). This indicates that more frequent observations are more useful for estimation of soil moisture and temperature profiles than knowledge of the near-surface observations for a greater period of time.

6.4.3.3 Kalman-Filtering

The results from simulations using the Kalman-filter assimilation scheme are given in Figure 6.27 for soil moisture and Figure 6.28 for soil temperature. In these figures, the assimilation of near-surface soil moisture and temperature observations for different soil moisture observation depths have different initial state variances. The reason for this was that the Kalman-filter assimilation scheme with daily updating was found to be more sensitive to the initial state variance for deeper observations.

For observation depths of 4 cm and 10 cm and an initial state variance of 1000000 (Figure 6.29), the Kalman-filter initially made a very poor update (negative improvement) of the soil moisture profile at the first update (day 1). At

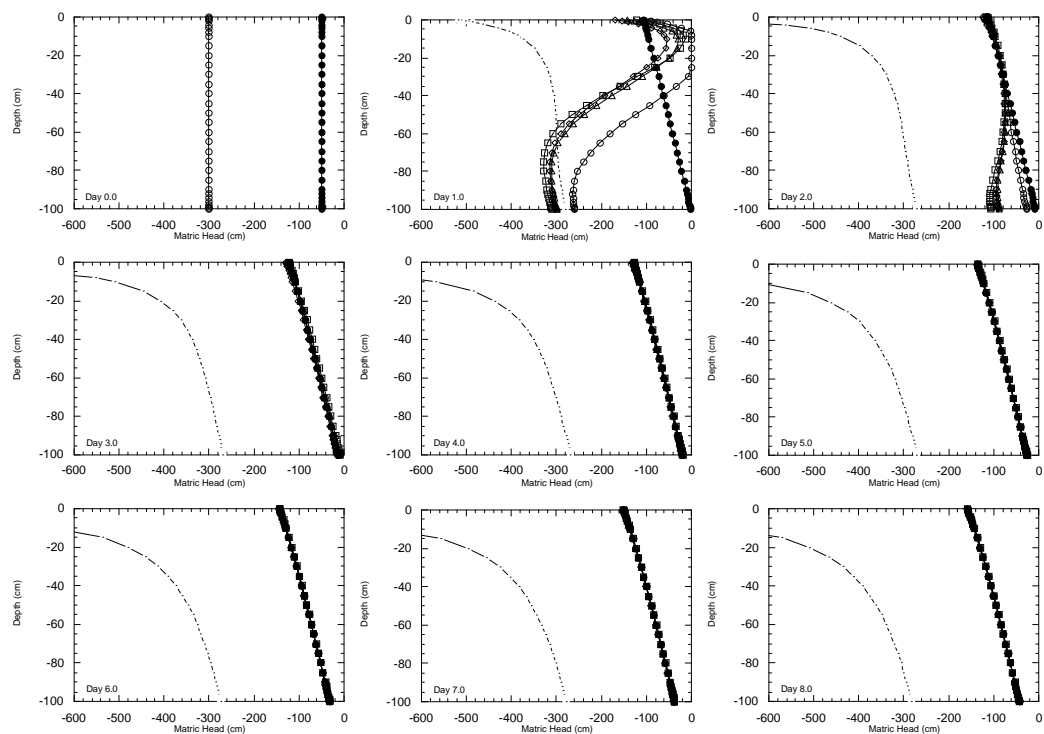


Figure 6.27: Comparison of soil moisture profile estimation using the Kalman-filter assimilation scheme for observation depths of 0 (open circle), 1 (open square), 4 (open triangle) and 10 cm (open diamond) with the “true” soil moisture profile (solid circle) and the open loop soil moisture profile (open circle with dot); initial state variances of 1000000, 1000000, 10000 and 1000 respectively. Observation variances 2% of observations and system noise 5% of change in states.

the next update (day 2), the Kalman-filter over-corrected for the previous poor update. This was also observed for estimation of the soil temperature profile with updating once every hour and zero observation noise (Figure 6.20), but the effect was not as severe.

To overcome this erratic updating of the soil moisture profile, the initial state variances were reduced until stable updates were obtained. The initial state variances required for this were 10000 for the observation depth of 4 cm and 1000 for 10 cm. Even though different initial state variances were used for the deeper observations, retrieval of the “true” soil moisture profile was achieved after approximately 3 days for all observation depths. However, improvement in soil moisture profile estimation for updating at the surface node alone occurred more quickly than for an observation depth of 1 cm, even though the same initial state variances were used. Retrieval of the “true” soil temperature profile occurred after approximately 6 days for all simulations. The different initial state variance appeared to have little effect on the improvements in estimation of the soil temperature profile, unlike the soil moisture profile. This may be due to the larger

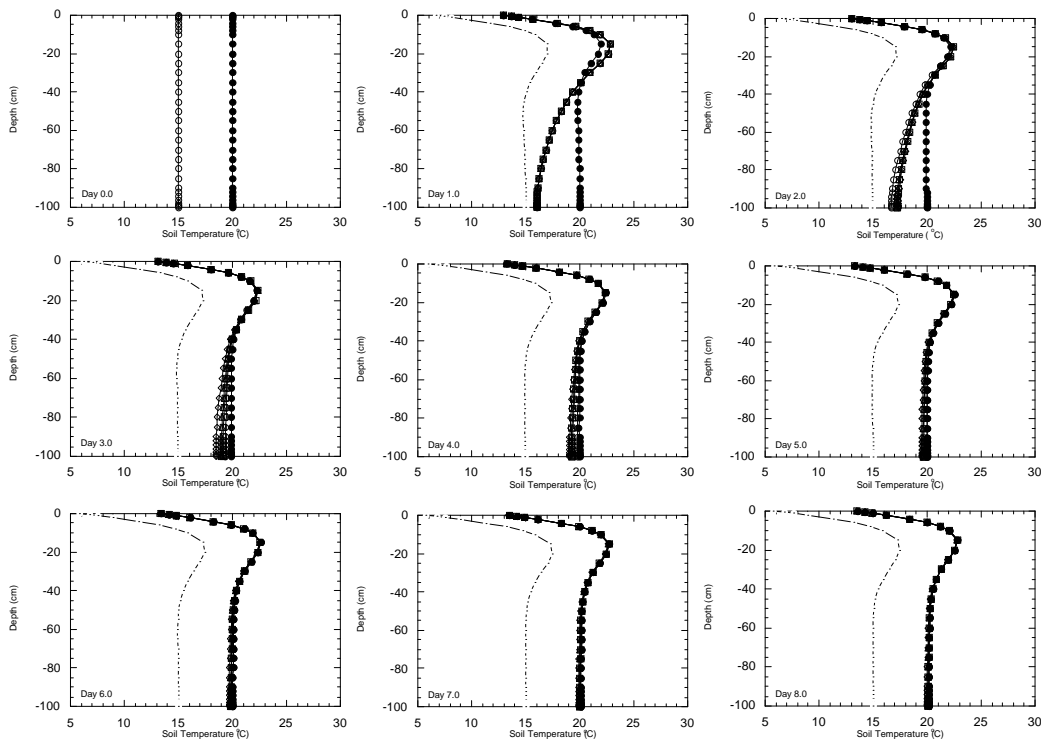


Figure 6.28: Comparison of soil temperature profile estimation using the Kalman-filter assimilation scheme for observations of the surface node (open symbols) with the “true” soil temperature profile (solid circle) and the open loop soil temperature profile (open circle with dot). Estimated soil temperature profiles correspond with soil moisture profile estimation for observations of 0 (open circle), 1 (open square), 4 (open triangle) and 10 cm (open diamond); initial state variances of 1000000, 1000000, 10000 and 1000 respectively. Observation variances 2% of observations and system noise 5% of change in states.

coefficient of variation for the soil temperature profile than for the soil moisture profile. These results are to be compared with more than 20 days for retrieval of the “true” soil moisture and temperature profiles using the hard-updating and a Dirichlet boundary condition.

As for hourly updating, the Kalman-filter assimilation scheme was superior to the hard-update assimilation scheme, both in terms of time required for retrieval of the “true” soil moisture and temperature profiles, and the effect of observation depth on improvements in soil moisture profile estimation. This highlights the benefit of the non mass-conservative nature of the Kalman-filter assimilation scheme, by making adjustments to the profile predictions for more than just the near-surface layer. However, unrealistic updating can occur with the Kalman-filter when observations become less frequent, the observed and modelled profiles are far apart, and there is large uncertainty in the model states. This again emphasises the importance of frequent observations.

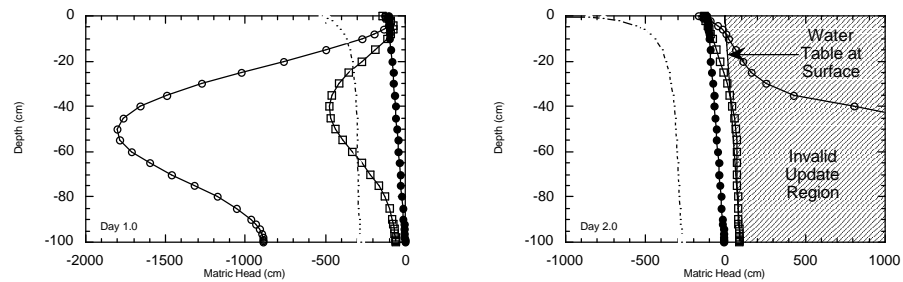


Figure 6.29: Comparison of soil moisture profile estimation using the Kalman-filter assimilation scheme with observation depths of 4 (open circle) and 10 cm (open square) with the “true” soil moisture profile (solid circle) and the open loop soil moisture profile (open circle with dot); initial state variance of 1000000. Observation variances 2% of observations and system noise 5% of change in states.

6.4.4 UPDATING ONCE EVERY FIVE DAYS

To test how infrequently near-surface observations could be made and still make satisfactory estimates of the soil moisture and temperature profiles, updating once every 5 days was examined.

6.4.4.1 *Hard-Updating and Dirichlet Boundary Condition*

Simulations using the hard-updating assimilation scheme with observations once every day showed the necessity for identifying a means of allowing extra soil moisture mass and heat energy to be added to or subtracted from the system, than that which the hard-updating could achieve on its own. In the simulations using daily observations, the addition or subtraction of soil moisture mass and heat energy was achieved by application of the Dirichlet boundary condition for 1 hour after the update. For 5 day updating, hard-updating alone would still be of little benefit in making improved estimates of the soil moisture and temperature profiles. Therefore, hard-updating was applied with a Dirichlet boundary condition for 1 hour after the update.

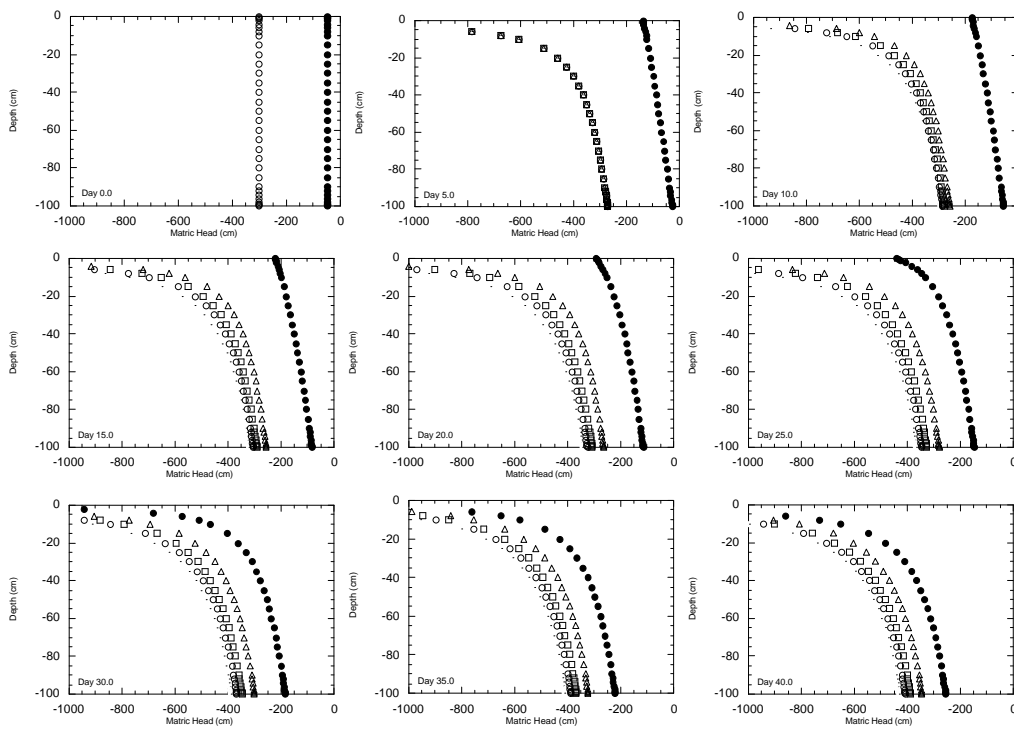


Figure 6.30: Comparison of soil moisture profile estimation using the hard-update assimilation scheme with a Dirichlet boundary condition for 1 hour over observation depths of 1 (open circle), 4 (open square) and 10 cm (open triangle) with the “true” soil moisture profile (solid circle) and the open loop soil moisture profile (open circle with dot).

6.4.4.1.1 Dirichlet Boundary Condition for One Hour

The hard-updating results with a Dirichlet boundary condition for 1 hour after updating are given in Figure 6.30 for soil moisture and Figure 6.31 for soil temperature. The results in Figure 6.30 indicate once again the benefit of an increased observation depth in the hard-update assimilation scheme. However, the advantage is much less pronounced than for previous simulations, with retrieval of the “true” soil moisture profile taking more than 40 days for all observation depths. Only minimal improvements in the soil moisture profile were achieved for an observation depth of 1 cm after 40 days. A more satisfactory improvement was obtained for the soil temperature profile, yet “true” and estimated soil temperature profiles still differed by approximately 5°C at depth, after 40 days.

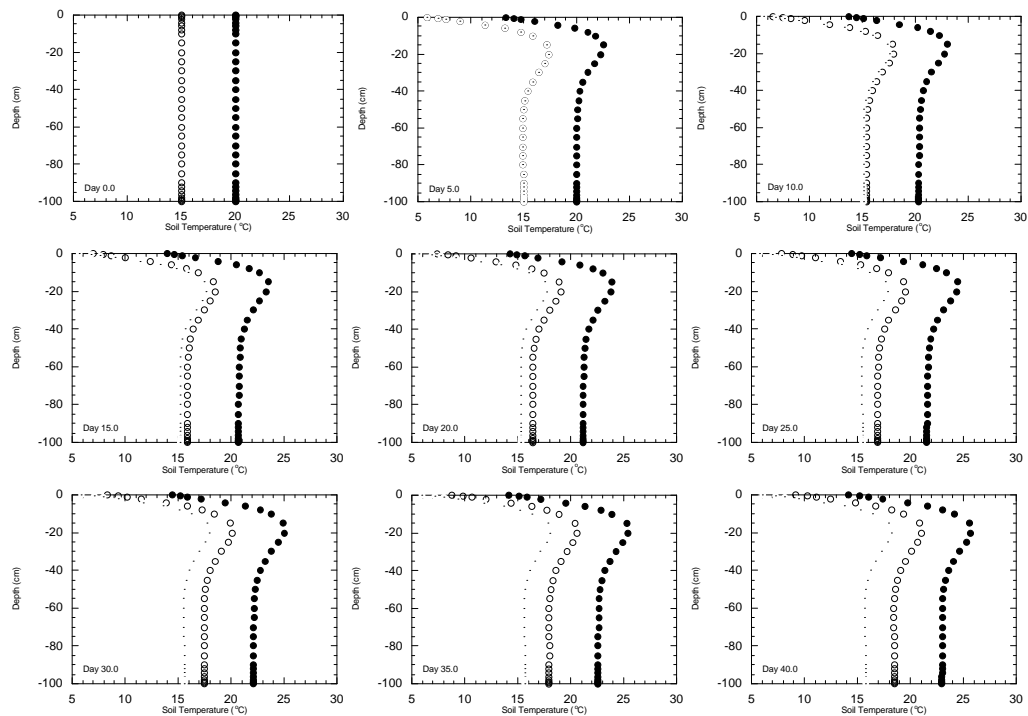


Figure 6.31: Comparison of soil temperature profile estimation using the hard-update assimilation scheme with a Dirichlet boundary condition for 1 hour at the surface node (open circle), with the “true” soil temperature profile (solid circle) and the open loop soil temperature profile (open circle with dot).

6.4.4.1.2 Dirichlet Boundary Condition for One Day

To further alleviate the soil moisture mass and heat energy balance problem, the Dirichlet boundary condition was applied for a period of 1 day after the update. The justification for this was that soil moisture does not change by more than a few percent during a day, unless it is raining. However, the soil surface temperature has a strong diurnal variation that needs to be accounted for. Thus, the “true” soil surface temperature values were used for modifying the Dirichlet boundary condition every hour (see Figure 6.5). The results from this simulation are given in Figure 6.32 for soil moisture and Figure 6.33 for soil temperature.

Both Figure 6.32 and Figure 6.33 show once again the advantage of knowing the “true” near-surface soil moisture and temperature values for a longer period of time. Using the Dirichlet boundary condition for a period of 1 day, retrieval of the “true” soil moisture profile was achieved after approximately 40 days for the 10 cm observation depth. Retrieval of the “true” soil temperature

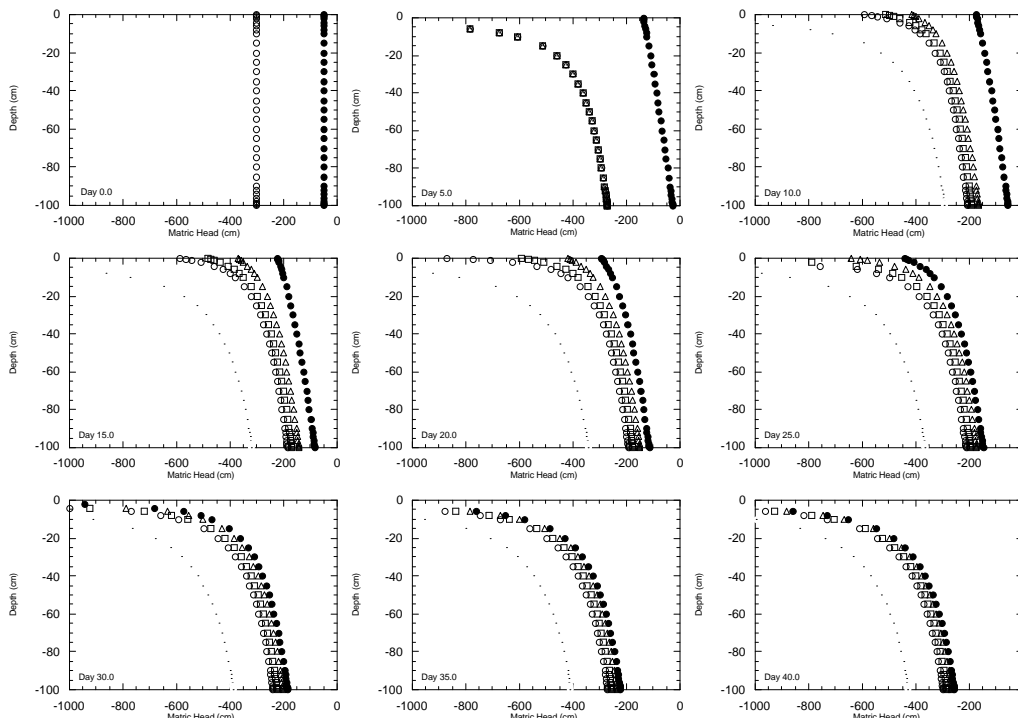


Figure 6.32: Comparison of soil moisture profile estimation using the hard-update assimilation scheme with a Dirichlet boundary condition for 1 day over observation depths of 1 (open circle), 4 (open square) and 10 cm (open triangle) with the “true” soil moisture profile (solid circle) and the open loop soil moisture profile (open circle with dot).

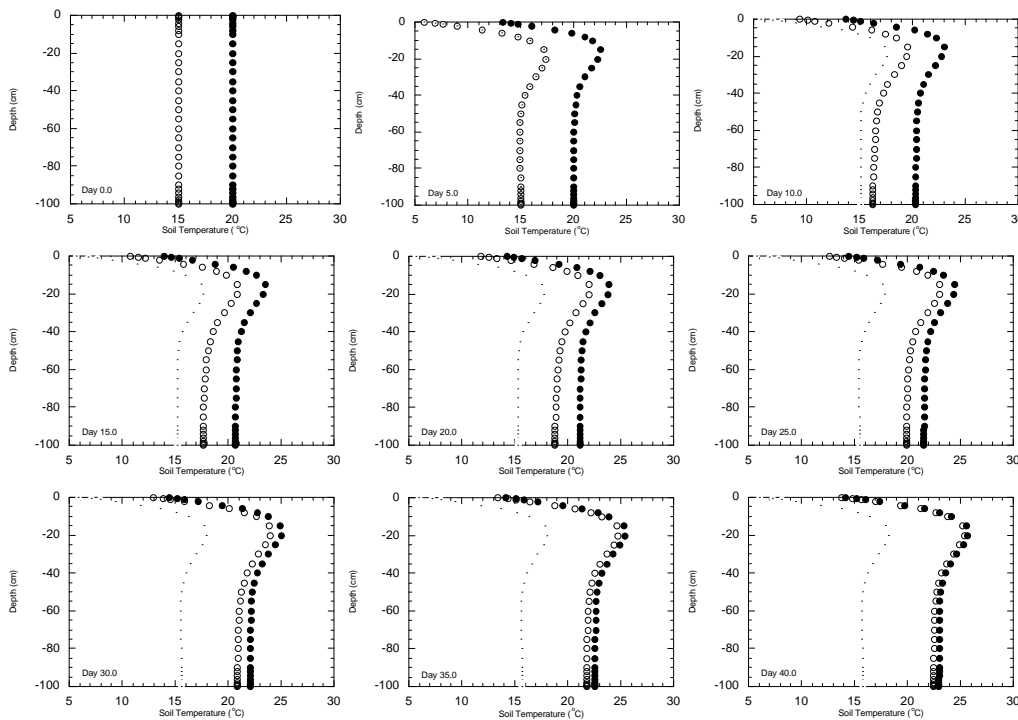


Figure 6.33: Comparison of soil temperature profile estimation using the hard-update assimilation scheme with a Dirichlet boundary condition for 1 day at the surface node (open circle) with the “true” soil temperature profile (solid circle) and the open loop soil temperature profile (open circle with dot).

profile also occurred after approximately 40 days, with “true” and estimated profiles differing by approximately 0.5°C at depth. These results are a significant improvement to those with a Dirichlet boundary condition for only 1 hour after the hard-update.

6.4.4.1.3 Sensitivity Analysis of the Dirichlet Boundary Condition

The improvement in soil moisture and temperature profile estimates using the hard-update assimilation scheme was determined by the length of time over which the continuous Dirichlet boundary condition was applied after the update, especially when the time between observations was increased. Hence, an investigation was undertaken to identify if there was a simple relationship between update interval and length of time for Dirichlet boundary condition, in order to achieve the same rate of improvement in soil moisture and temperature profile estimates. To investigate this, the Dirichlet boundary condition was applied for a fixed proportion of the update interval. Thus, hard updates were made every 1 day, 2 days and 4 days, with a Dirichlet boundary condition for 1 hour, 2 hours and 4 hours respectively. The results from these simulations are given in Figure 6.34 for soil moisture and Figure 6.35 for soil temperature.

The simulations in both Figure 6.34 and Figure 6.35 show conclusively

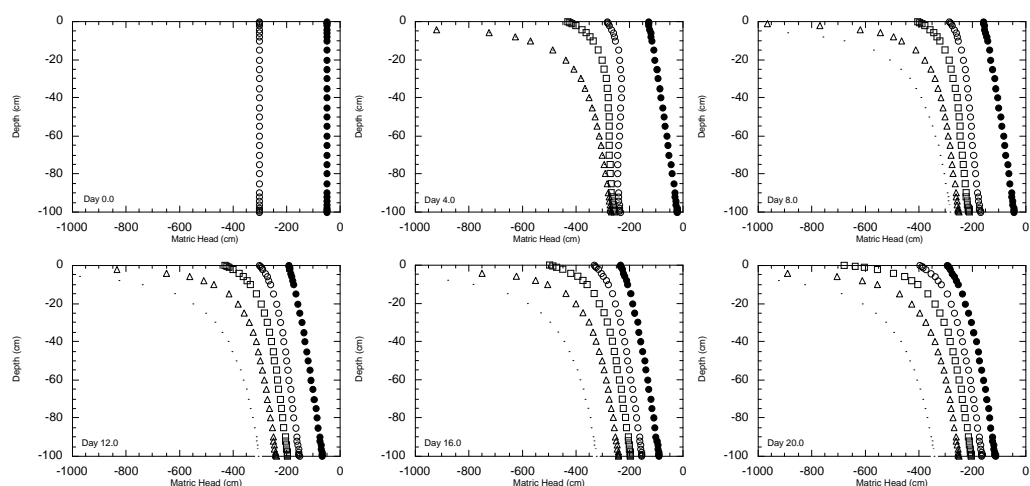


Figure 6.34: Comparison of soil moisture profile estimation using the hard-update assimilation scheme with a Dirichlet boundary condition over an observation depth of 4 cm (open symbols) with the “true” soil moisture profile (solid circle) and the open loop soil moisture profile (open circle with dot). Update every day and Dirichlet boundary condition for 1 hour (open circle), update every 2 days and Dirichlet boundary condition for 2 hours (open square), and update every 4 days and Dirichlet boundary condition for 4 hours (open triangle).

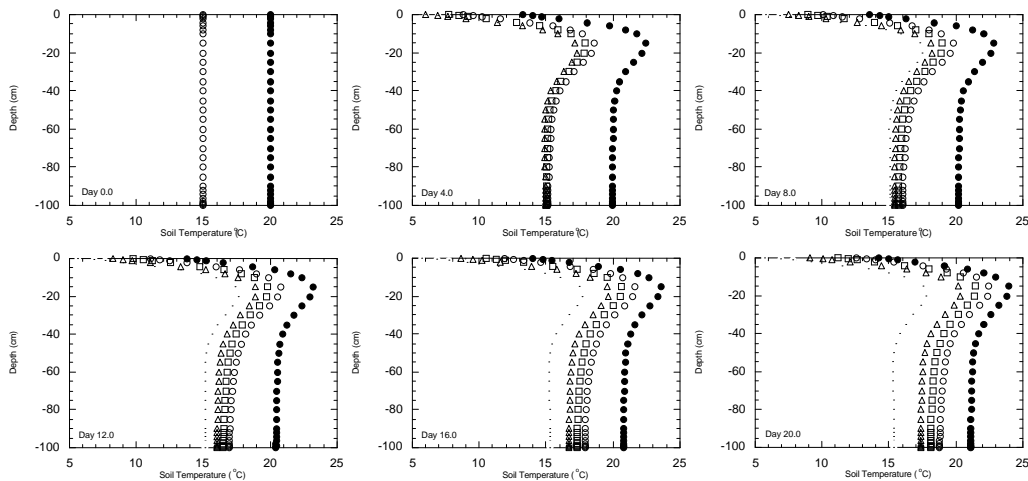


Figure 6.35: Comparison of soil temperature profile estimation using the hard-update assimilation scheme with a Dirichlet boundary condition at the surface node (open symbols) with the “true” soil moisture profile (solid circle) and the open loop soil moisture profile (open circle with dot). Update every day and Dirichlet boundary condition for 1 hour (open circle), update every 2 days and Dirichlet boundary condition for 2 hours (open square), and update every 4 days and Dirichlet boundary condition for 4 hours (open triangle).

that the relationship between update interval and the proportion of that interval for which a Dirichlet boundary condition must be applied in order to achieve the same rate of improvement in soil moisture and temperature profile estimation using the hard-update assimilation scheme was not constant. In fact, it was found that as the interval between observations was increased, knowledge of the “true” near-surface soil moisture and temperature was required for a greater proportion of the update interval. This again highlights the greater importance of more frequent observations than the length of time for which knowledge of the “true” surface states are available.

6.4.4.2 Kalman-Filtering

Initial simulations with the Kalman-filter assimilation scheme used the same initial state variance, model noise and observation noise as used in hourly and daily updating simulations (initial state variance of 1000000, system noise 5% of change in states and observation noise 2% of observations). This however, yielded poor updates of the soil moisture profile, as shown in Figure 6.36 for a 1 cm observation depth (open square). Rather than perform an update which lay somewhere between the “true” and open loop profiles, the updated soil moisture profile was equal to the “true” soil moisture profile at the soil surface, followed by an oscillation between the open loop soil moisture profile and zero matric head,

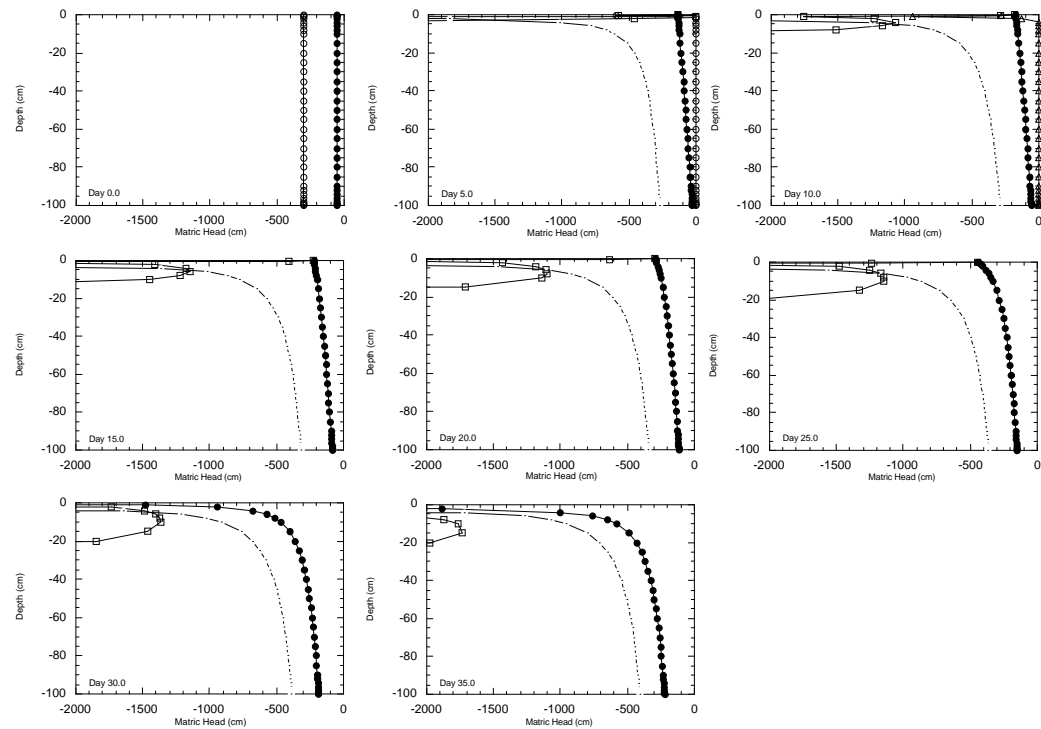


Figure 6.36: Comparison of soil moisture profile estimation using the Kalman-filter assimilation scheme for an observation depth of 1 cm with the “true” soil moisture profile (solid circle) and the open loop soil moisture profile (open circle with dot). Initial state variances of 1000 (open circle), 1000000 (open square) and 1e12 (open triangle); system noise 5% of change in states and observation noise 2% of observations.

before shooting off to a very negative matric head. In subsequent updates there was a movement of the estimated soil moisture profile towards the “true” soil moisture profile at deeper depths. However, this movement was slow and the estimated soil moisture profile was still further from the “true” soil moisture profile than the open loop profile after 35 days. This is different to that observed earlier with daily updating, where the Kalman-filter recognised its mistake in the first update and over-corrected in the second update.

It is well known that the extended Kalman-filter often diverges from the “true” solution if the initial estimate is not sufficiently good or the non-linearities are severe, and that the behaviour of the extended Kalman-filter is often worse when the model error is large and/or the inputs are small (Ljung, 1979). Hence, in practical applications of the extended Kalman-filter, “manual” adjustments of the noise covariances are often used to make the algorithm work, and is referred to as “tuning of the filter” (Ljung, 1979). In the daily updating, these stability problems were overcome by reducing the initial state variance (“tuning” of the filter).

Hence, a sensitivity analysis was undertaken to see if the Kalman-filter updates could be improved by “tuning”.

6.4.4.2.1 Sensitivity Analysis of the Initial State Variance

The simulation described in the previous section was re-run with an initial state variance of 1000. The effect of this is shown in Figure 6.36 (open circles), with the first soil moisture profile update being equal to the “true” soil moisture profile at the soil surface, followed by an oscillation towards the open loop profile before shooting off towards a large positive matric head, which was constrained to zero. Figure 6.36 also shows the effect of increasing the initial state variance to $1e12$ (open triangle), where the first soil moisture profile update was equal to the “true” soil moisture profile at the soil surface, before shooting off to a very large negative matric head. Unlike the simulation with an initial state variance of 1000000, the Kalman-filter realised its mistake at the first update, and over-corrected at the second update (day 10), with the updated soil moisture profile being equal to the “true” soil moisture profile at the soil surface, followed by an oscillation towards the open loop profile before shooting off towards a large positive matric head, which was constrained to zero.

By further reducing the initial state covariances, it was possible to obtain reasonable updates of the soil moisture profile (Figure 6.37). In order to achieve this, initial state variances were reduced to 10, 5 and 15 for observation depths of 1, 4 and 10 cm respectively. By reducing the initial state variances to such low values forced the Kalman-filter to perform its updates much more cautiously, as previously illustrated in Figure 6.15. Thus, retrieval of the “true” soil moisture profile was achieved after approximately 30 days for the 10 cm observation depth. However, the improvement in soil moisture profile estimates for shallower observation depths proceeded more slowly, most likely as a result of the smaller initial state variances. It should also be noted that for these simulations, the progression in improvement of soil moisture profile estimation towards the “true” soil moisture profile occurred from the base of the soil column, which is similar to that observed in the work by Entekhabi *et al.* (1994).

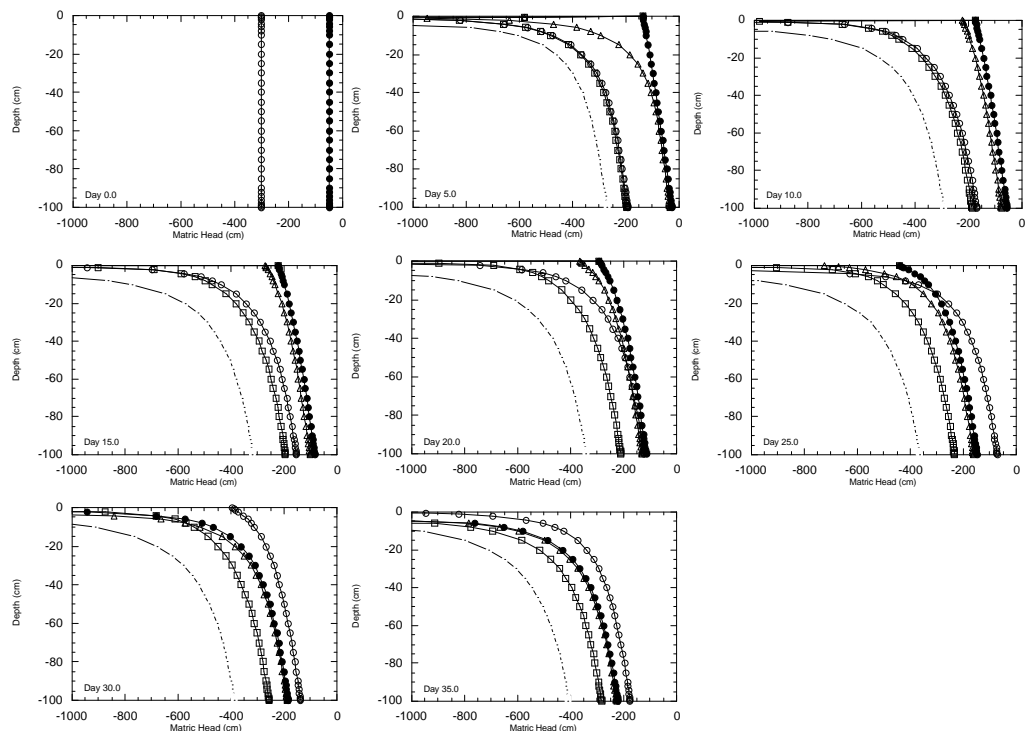


Figure 6.37: Comparison of soil moisture profile estimation using the Kalman-filter assimilation scheme over depths of 1 (open circle), 4 (open square) and 10 cm (open triangle) with the “true” soil moisture profile (solid circle) and the open loop soil moisture profile (open circle with dot). Initial state variances for the estimated soil moisture profiles were 10, 5 and 15 respectively; system noise 5% of change in states and observation noise 2% of observation.

6.4.4.2.2 Sensitivity Analysis of the Initial Update

Using such extremely small values for the initial state variance indicated to the Kalman-filter a high degree of confidence in the initial guess, which was obviously untrue. Furthermore, there was a strong dependence on the initial state variance for satisfactory updating of the soil moisture profile, resulting in large differences in the efficiency of soil moisture profile estimation for slight changes in the initial state variance.

These two factors initiated a search for a more robust application of the Kalman-filter assimilation scheme. The first option was to introduce an extra update shortly after the commencement of the simulation. The reason for this was: (i) it was felt that if the model prediction was closer to the observation (as with the soil temperature profile) the updating of the soil moisture profile would be more robust; (ii) an early update would move the estimated soil moisture profile closer to the “true” soil moisture profile (at least in the near-surface soil nodes), resulting in the model prediction being closer to the observations at the first update; and

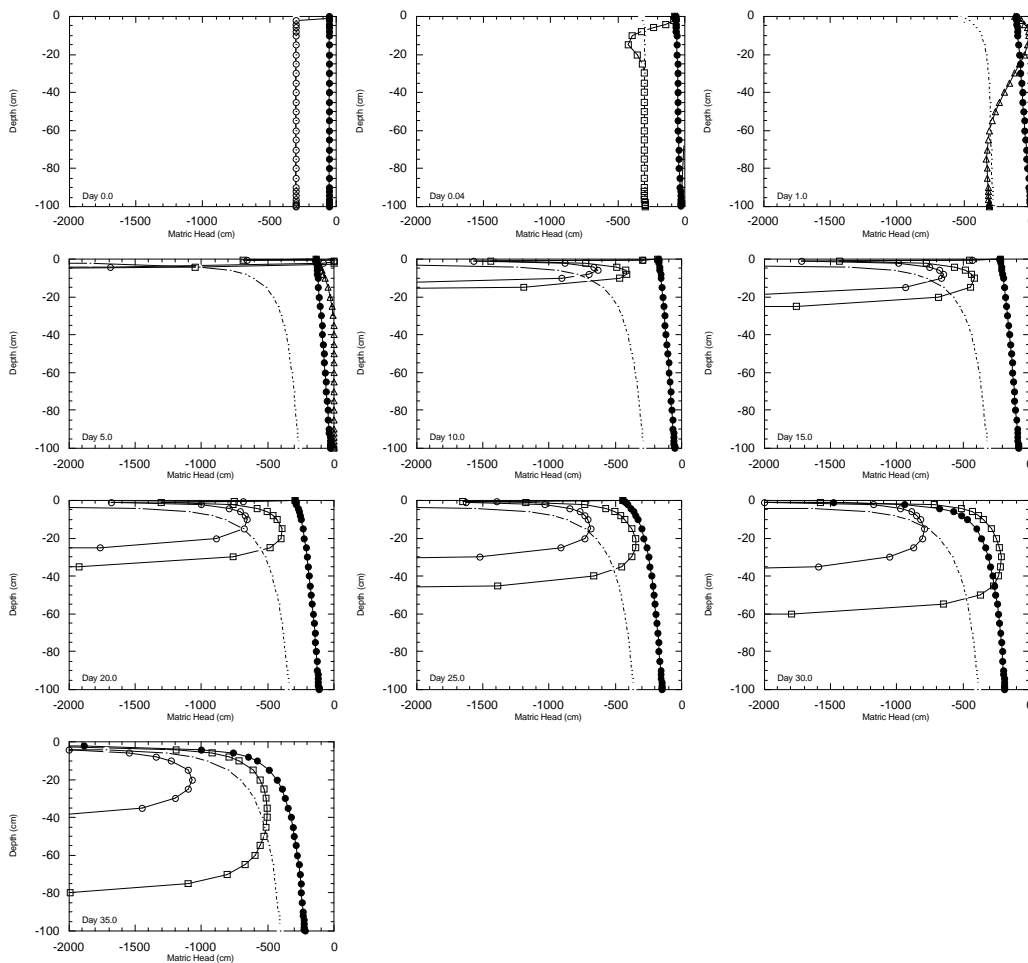


Figure 6.38: Comparison of soil moisture profile estimation using the Kalman-filter assimilation scheme for an observation depth of 1 cm with the “true” soil moisture profile (solid circle) and the open loop soil moisture profile (open circle with dot). First update at time 0 hours (open circle), 1 hour (open square) and 1 day (open triangle); initial state variances 1000000, system noise 5% of change in states and observation variances 2% of observations.

(iii) in a real life application, simulations of soil moisture would commence with an initial soil moisture profile that was equal to the “true” soil moisture profile for at least the near-surface nodes, resulting in the model prediction being closer to the observations at the first update. Thus, preliminary updates were made at time zero, 1 hour and 1 day.

The results from these simulations are given in Figure 6.38, where it can be seen that the update at time zero simply replaced the poor initial soil moisture profile guess with the “true” initial soil moisture profile values over the observation depth. This was as expected, as there were no cross-correlations in the initial covariance matrix, which control the updating at deeper depths. The update at 1 hour made an adjustment to slightly deeper depths in the soil profile, as the

Kalman-filter had time to build up cross-correlations among the near-surface nodes. Due to the extra time lapse for the initial update at day 1, the Kalman-filter was able to make a much larger adjustment to the soil moisture profile. However, the Kalman-filter still made an over-adjustment to the soil moisture profile estimate at day 5. The subsequent updates, for preliminary updates at time zero and 1 hour, show similar characteristics to that of having no preliminary update (Figure 6.36). However, there was a greater movement towards the “true” profile than there was for no preliminary update, with the effect being greater for the preliminary update at day 1. Even after seven updates (day 35) the soil moisture profile estimate did not agree closely with the “true” soil moisture profile.

6.4.4.2.3 Sensitivity Analysis of the System Noise

Another factor that could affect soil moisture profile updates with the Kalman-filter was the system noise. When the Kalman-filter makes an update of the system states, it reduces the magnitude of the covariances of the system state. Thus for further observations to be beneficial, it is necessary to increase the system state covariances above the observation noise, during the forecasting period. The slow improvement of the poor soil moisture profile update with an initial state variance of 1000000 (Figure 6.36) may be indicative of too little noise in the system. To identify if adding extra noise would improve the soil moisture profile estimation, three different system noises were investigated: (i) 10% of change in system states during the time step; (ii) 5% of the maximum change in system state over the profile during the time step; and (iii) 5% of the system state normalised by the time step size (ie. 5% of the system state per hour).

The results of these simulations are given in Figure 6.39, where it can be seen that increasing the system noise to 10% of the change in system states during the time step had a significant effect on the soil moisture profile estimate at the second update (day 10). The soil moisture profile estimate at day 10 was the same as for the “true” soil moisture profile at the soil surface, oscillated towards the open loop profile, and then back to zero matric head before shooting off to a not quite so negative matric head at the base of the soil column. The Kalman-filter then over-corrected at the third update (day 15). The remaining two system noise

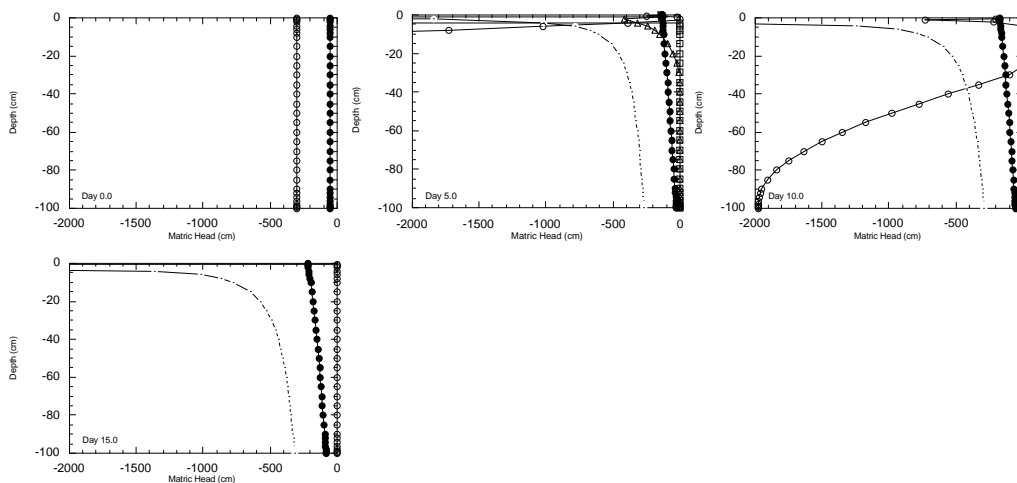


Figure 6.39: Comparison of soil moisture profile estimation using the Kalman-filter assimilation scheme for an observation depth of 1 cm with the “true” soil moisture profile (solid circle) and the open loop soil moisture profile (open circle with dot). System noise was 10% of change in states (open circle), 5% of maximum change in states (open square) and 5% of states per hour (open triangle); initial state variances 1000000 and observation variances 2% of observations.

scenarios investigated, resulted in the Kalman-filter over-correcting at the first update.

6.4.4.2.4 Quasi Observations in the Kalman-Filter

Given the failure of all obvious measures (ie. “tuning” of the filter) for increasing the robustness of the Kalman-filter assimilation scheme, a new approach was sought. Near-surface observations of soil moisture content are indicative of the soil moisture content at depth (see Chapter 3). Thus it was proposed to apply both the actual observations over the observation depth, and “quasi” observations to the remainder of the soil profile. This is illustrated in Figure 6.40.

The quasi observations could either be: (i) the observed soil moisture at the observation depth; or (ii) an extrapolation of the soil moisture observation at the observation depth by the steady state assumption. Under this assumption, the laws of physics state that all points in the soil profile must have the same hydraulic potential, which is the summation of the hydraulic potential and the gravitational potential (ie. $\psi + z = \text{constant}$, see also section 3.4.2). It was chosen to apply the steady state assumption, as this has been shown to be a reasonable approximation under low flux conditions (Jackson, 1980). In addition, when there

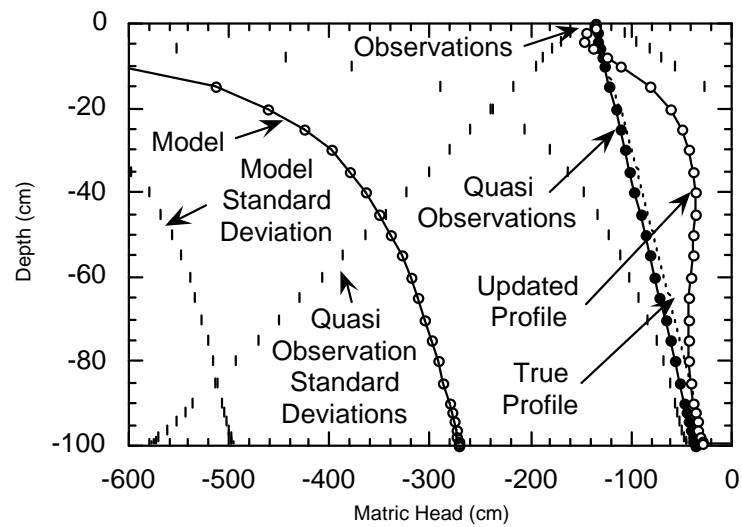


Figure 6.40: Illustration of the Kalman-filter assimilation scheme using quasi observations.

is a large matric head gradient under exfiltration conditions, this would have the effect of making the quasi observations slightly closer to reality.

There is much greater uncertainty associated with a quasi observation than for the actual observations, even for a layer of soil directly below the observation depth. With increasing depth from the lowest observation, the uncertainty in the quasi observation increases dramatically. To account for this, a quantile jump was applied to the variance of the quasi observation immediately below the observation depth, relative to the variance of the actual observations. An increasing quasi observation variance was then applied with depth.

Two scenarios were used to initially test the Kalman-filter assimilation scheme with quasi observations: (i) quasi observation noise varying from 5% of the quasi observation to 100% of the quasi observation; and (ii) quasi observation noise varying from 5% of the lowest observation to 100% of the lowest observation. The results from these simulations are given in Figure 6.41, where it can be seen that both scenarios resulted in a poor estimate of the soil moisture profile at the first update. At the second update, the soil moisture profile estimate for the first scenario went to a large negative value at the surface node while the remainder of the profile went to zero. This was due to the observation variances being much larger than the system state variances, as a result of insufficient noise in the system (5% of change in states), especially at deeper depths where there

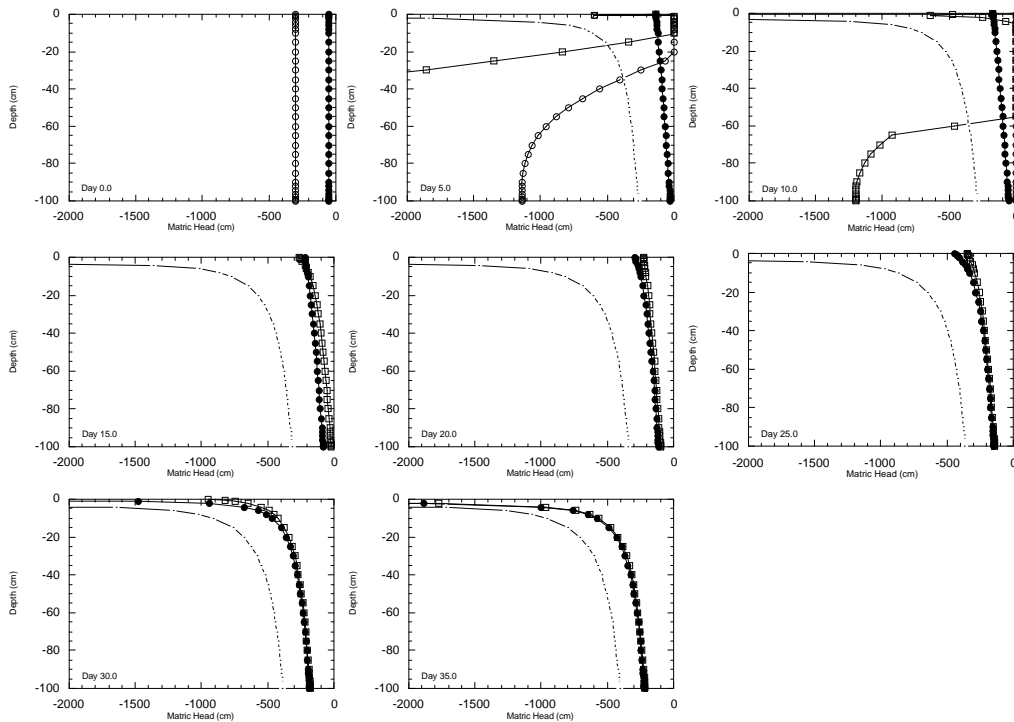


Figure 6.41: Comparison of soil moisture profile estimates using the Kalman-filter assimilation scheme for an observation depth of 1 cm with the “true” soil moisture profile (solid circle) and the open loop soil moisture profile (open circle with dot). Quasi observations were applied to the remainder of the profile with observation variances varying from 5% to 100% of the quasi observation (open circle) and 5% to 100% of the lowest observation (open square); initial state variances 1000000, observation variances 2% of observations and system noise 5% of change in states.

was not much change in the matric head with time. The updated soil moisture profile for the second scenario managed to just survive the second update and then started to become reasonable at the third update. This survival of the second update was felt to be more good luck than an attribute of the quasi observation variance. A lack of system noise can also be seen at day 20 and day 25, where the soil moisture profile estimate for the second scenario did not go to the observed soil moisture content for the near-surface nodes.

In order to verify that the poor estimates of the soil moisture profile in the previous simulations were due to a lack of system noise, the simulation was repeated for a system noise of 5% of the states per hour. In this simulation, only the second scenario was used, as the first scenario was a misrepresentation of the desired quasi observation variance. By applying the steady state assumption for quasi matric head observations, the “observed” matric head is decreasing with depth. Thus, unless the increase in percentage of state for quasi observations is large enough, it is possible for a net decrease in quasi observation variance with

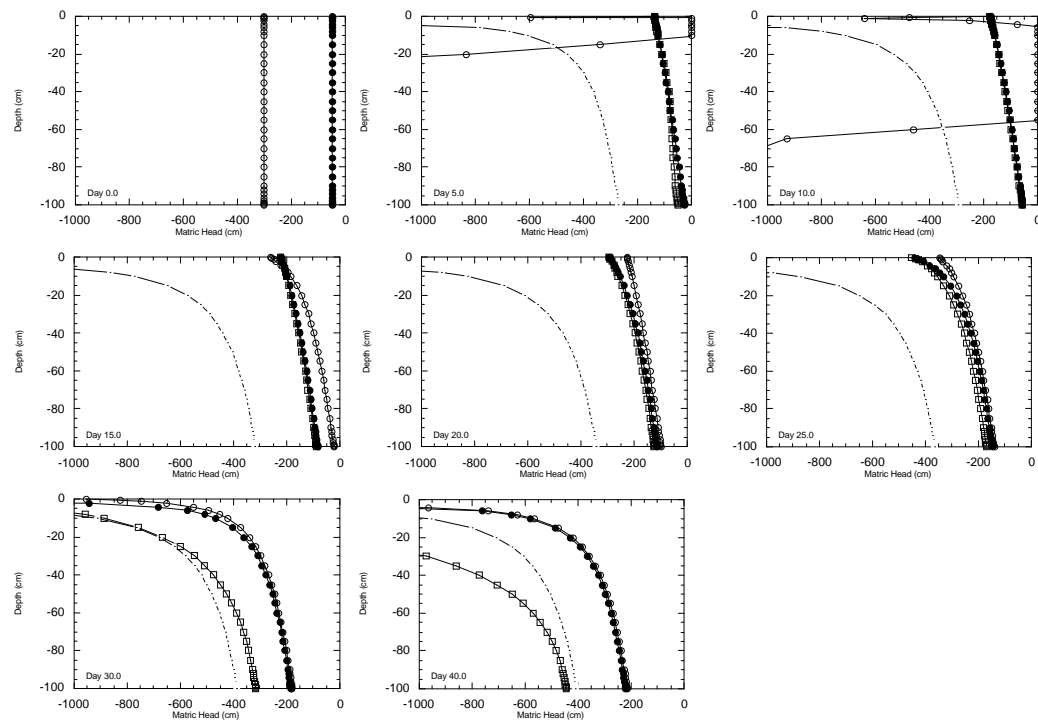


Figure 6.42: Comparison of soil moisture profile estimation using the Kalman-filter assimilation scheme for an observation depth of 1 cm with the “true” soil moisture profile (solid circle) and the open loop soil moisture profile (open circle with dot). Quasi observations were applied to the remainder of the soil profile with observation variances varying from 5% to 100% of the lowest observation; system noise 5% of change in states (open circle) and 5% of states per hour (open square); initial state variances 1000000 and observation variances 2% of observations.

depth, as was the case with the first scenario. Using the second scenario ensures that there is a net increase in quasi observation variance with depth. Furthermore, it makes better sense to determine the variance of the quasi observations a function of the soil moisture value used to estimate the quasi observation.

The results of this second simulation are given in Figure 6.42, where it can be seen that the increased system noise resulted in the Kalman-filter making a good estimate of the “true” soil moisture profile after the first update. The soil moisture profile estimate then continued to follow the “true” soil moisture profile through to approximately day 25, where it started to move towards the open loop profile. This can be seen more distinctly at day 30 and day 35, and was a result of the poor quasi observations for these updates. At these updates, the matric head was very largely negative at the soil surface and had a steep matric head gradient with depth, being far from the steady state condition. Thus the quasi observations at deeper depths were far from the “true” soil moisture profile. As a result of the quasi observation variances being too small compared to the variances of the

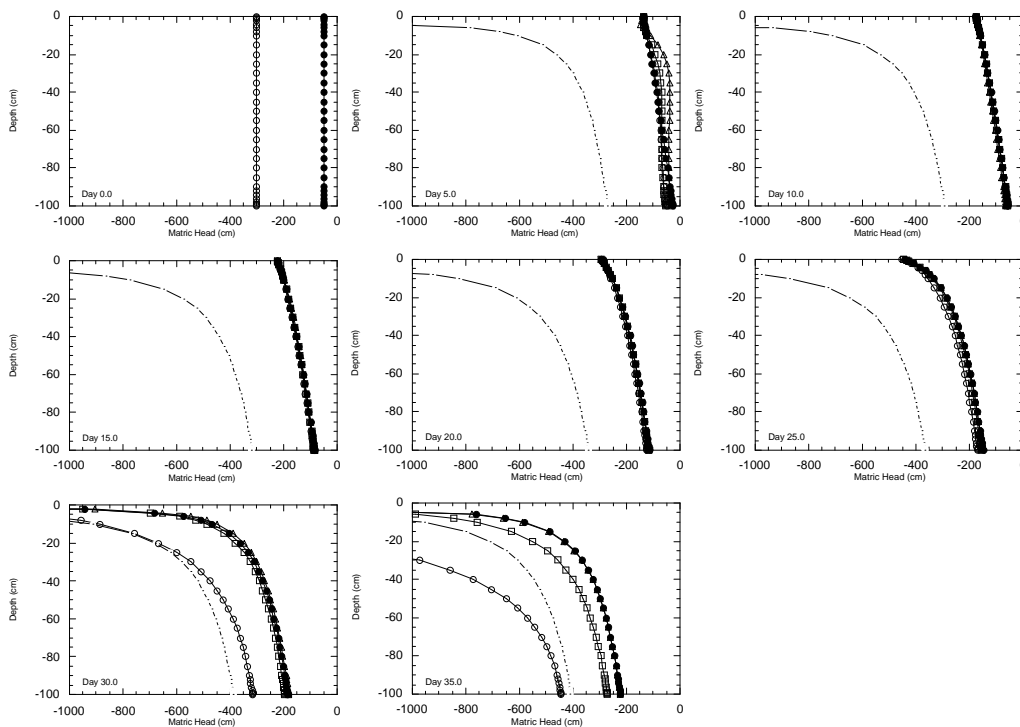


Figure 6.43: Comparison of soil moisture profile estimation using the Kalman-filter assimilation scheme for an observation depth of 1 cm with the “true” soil moisture profile (solid circle) and the open loop soil moisture profile (open circle with dot). Quasi observations are applied to the remainder of the soil profile with observation variances varying from 5% to 100% (open circle), 10% to 200% (open square) and 20% to 400% (open triangle) of the lowest observation; initial state variances 1000000, observation variances 2% of observations and system noise 5% of states per hour.

forecast system states, the Kalman-filter placed increasingly more faith in the quasi observations than in the forecast system states, thus moving its best estimate towards the quasi observations.

To overcome the problem with poor quasi observations at later updates, simulations were run with increased variances on the quasi observations. The variances that were used varied linearly from: (i) 10% of the lowest observation to 200% of the lowest observation; and (ii) 20% of the lowest observation to 400% of the lowest observation. These results are compared in Figure 6.43 with the simulation using a quasi observation variance that varied linearly from 5% of the lowest observation to 100% of the lowest observation.

These simulations show that with the increased quasi observation variance, an extra update was required in order to retrieve the “true” soil moisture profile. However, the increased quasi observation variance alleviated the effect of poor quasi observations on estimation of the soil moisture profile after the “true” soil

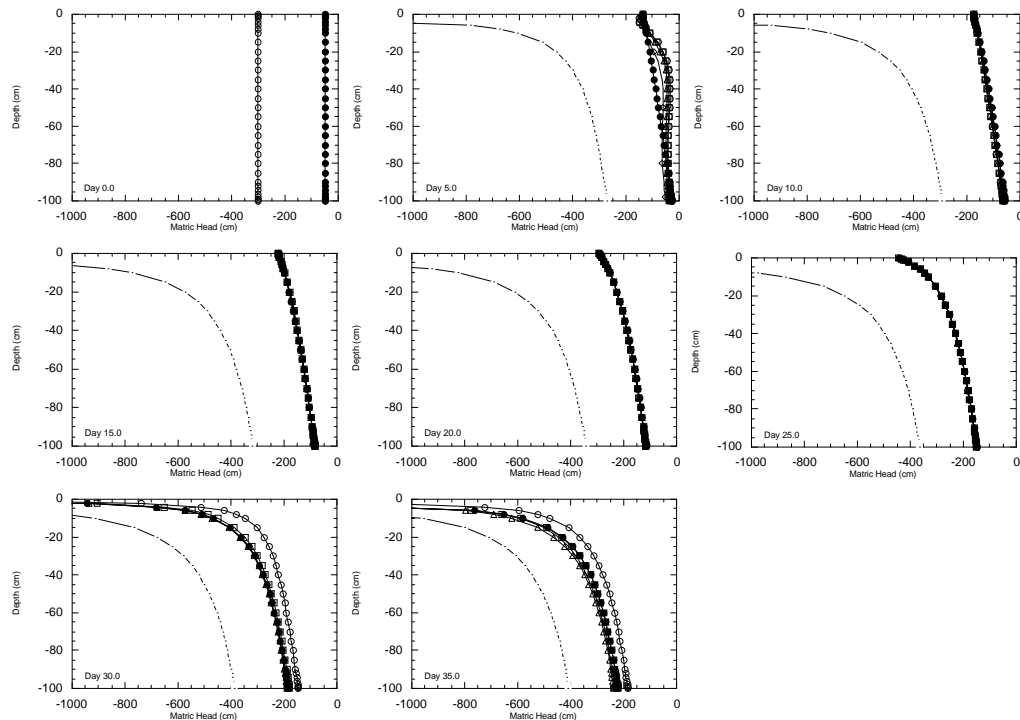


Figure 6.44: Comparison of soil moisture profile estimation using the Kalman-filter assimilation scheme for observation depths of 0 (open circle), 1 (open square), 4 (open triangle) and 10 cm (open diamond) with the “true” soil moisture profile (solid circle) and the open loop soil moisture profile (open circle with dot); quasi observations were applied over the remainder of the soil profile with variances varying from 20% to 400% of the lowest observation. Initial state variances of 1000000, observation variances 2% of observations and system noise 5% of states per hour.

moisture profile was correctly retrieved, particularly for the larger quasi observation variances.

Given a soil moisture profile estimation algorithm that reliably estimated the soil moisture profile for the 1 cm observation depth, we were in the situation where we could test it for other observation depths. The results from these simulations are given in Figure 6.44 for soil moisture and Figure 6.45 for soil temperature.

These results show that the “true” soil moisture profile was retrieved after only 10 days (two updates) whilst retrieval of the “true” soil temperature profile occurred after only 15 days. This is to be compared with 40 days for retrieval of soil moisture and temperature profiles using the hard-update assimilation scheme with an observation depth of 10 cm and Dirichlet boundary condition for 1 day, again showing the advantage of the Kalman-filter. However, the Kalman-filter was not without its problems. Once retrieval of the “true” soil moisture profile was achieved, the profile estimation algorithm continued to track the “true” soil

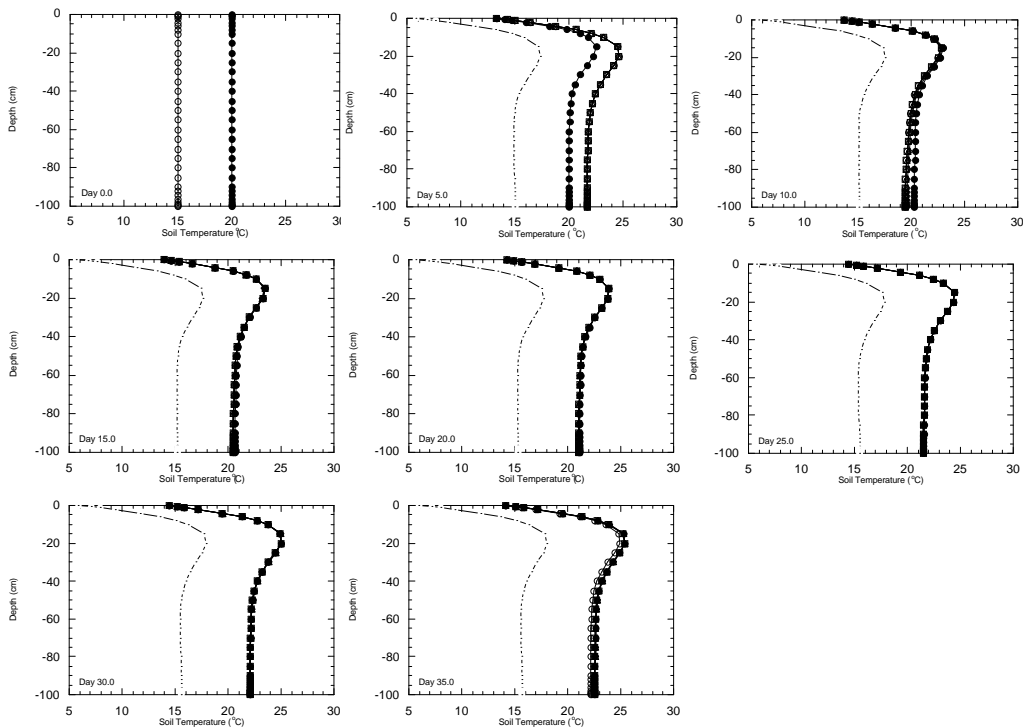


Figure 6.45: Comparison of soil temperature profile estimates using the Kalman-filter assimilation scheme for observations of the surface node (open symbols) with the “true” soil temperature profile (solid circle) and the open loop soil temperature profile (open circle with dot). Soil temperature profiles correspond with soil moisture profile estimation for observation depths of 0 (open circle), 1 (open square), 4 (open triangle) and 10 cm (open diamond); initial state variances of 1000000, observation variances 2% of observations and system noise 5% of the states per hour.

moisture profiles until day 30. At this time, estimates of the soil moisture profile using observations of the surface node began to depart from the “true” soil moisture profile. This was again caused by the departure of the “true” soil moisture profile from steady state and the extremely large negative matric head at the soil surface. Under field conditions the situation would most likely be somewhat different, as evaporation would not be occurring at a constant rate, allowing for capillary rise during periods of low evaporation. Thus, this departure from the “true” profile at later updates did not warrant any major concern, as this would be an extreme situation.

The main focus in this section of the synthetic study was to make satisfactory updates with the Kalman-filter during the initial stages of soil moisture and temperature profile estimation. The reason this may have been possible with the quasi observations in these simulations, is that the “true” profile was approximately steady state during the early updates. Only a field application will truly reveal if this is the situation. However, providing the model is initialised

at an appropriate time (ie. period of saturation) this should not be an issue for application of the soil moisture profile estimation algorithm using the Kalman-filter assimilation scheme.

6.4.4.2.5 Log Transformation in the Kalman-Filter

Whilst it was necessary to apply quasi observations to the unobserved portion of the soil moisture profile in order to provide stability to Kalman-filter updates with observations every 5 days, soil temperature profile updates did not exhibit any of these problems when using only the surface node observations. It would appear from this that providing the observations are not too far from the forecast system states, the Kalman-filter can provide a stable update. Thus, if we can possibly reduce the difference between the observed and forecast soil moisture values, we may be able to estimate the moisture profile using only the soil moisture observations over the observation depth. One way in which this reduction in difference between observed and simulated near-surface soil moisture can be achieved is through a log transformation of the matric head. This is illustrated in Figure 6.46.

In order to apply this transformation, both the observations and forecast system states, and their covariances, must be transformed into log space. These transformations may be achieved through the relationships (Bras and Rodriguez-Iturbe, 1985)

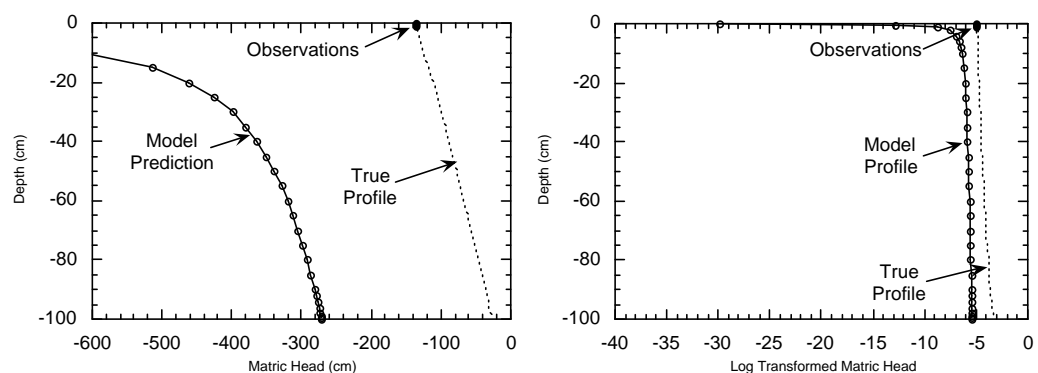


Figure 6.46: Illustration of reduction in difference between observed and measured near surface soil moisture using a log transformation of the matric head.

$$\mu_{X'_i} = \log_e(\mu_{X_i}) - \frac{\sigma_{X'_i}^2}{2} \quad (6.2a)$$

$$\sigma_{X'_i} = \log_e \left(\frac{\sigma_{X'_i}^2}{\mu_{X'_i}^2} + 1 \right) \quad (6.2b)$$

$$\rho_{X'_i X'_j} = \frac{\log_e \left(1 + \rho_{X_i X_j} \sqrt{(\exp\{\sigma_{X'_i}^2\} - 1)(\exp\{\sigma_{X'_j}^2\} - 1)} \right)}{\sigma_{X'_i} \sigma_{X'_j}} \quad (6.2c)$$

$$\rho_{X'_i X_j} = \frac{\rho_{X_i X_j} \sqrt{(\exp\{\sigma_{X'_i}^2\} - 1)}}{\sigma_{X'_i}} \quad (6.2d),$$

where X_i and X_j are the i th and j th states in the original system with mean μ , standard deviation σ and correlation coefficient ρ . X'_i and X'_j are the i th and j th states in the log transformed system. As the Kalman-filter tracks the conditional mean of the system, the means of the original system are the forecast system states.

After the system update, the updated system states and their covariances must be transformed back into the original system. These transformations may be achieved through the relationships (Bras and Rodriguez-Iturbe, 1985)

$$\mu_{X_i} = \exp \left\{ \frac{\sigma_{X'_i}^2}{2} + \mu_{X'_i} \right\} \quad (6.3a)$$

$$\sigma_{X_i}^2 = \exp \left\{ 2 \left[\sigma_{X'_i}^2 + \mu_{X'_i} \right] \right\} - \exp \left\{ \sigma_{X'_i}^2 + 2\mu_{X'_i} \right\} \quad (6.3b)$$

$$\rho_{X_i X_j} = \frac{\exp\{\sigma_{X_i} \sigma_{X_j} \rho_{X_i X_j}\} - 1}{\exp\{\sigma_{X_i}^2\} - 1} \quad (6.3c)$$

$$\rho_{X_i X_j} = \frac{\rho_{X_i X_j} \sigma_{X_i}}{\sqrt{(\exp\{\sigma_{X_i}^2\} - 1)}} \quad (6.3d)$$

Using the log transformation, stable updates of the soil moisture profile were achieved using the 1 cm observation depth without quasi observations, for an initial state variance of 1000000, system state noise of 15% of the states per hour, and an observation noise of 2% of the observations. The results from this simulation are given in Figure 6.47, where it can be seen that the soil moisture profile estimate coincided with the “true” soil moisture profile after approximately 10 days. Once the “true” soil moisture profile was retrieved, the soil moisture profile estimation algorithm continued to track the “true” soil moisture profile. However, the first update (day 5) was very sensitive to the initial state variance and system state noise, with other values resulting in the same unstable updates shown in previous sections. In addition, the combination of initial state variance and system noise required for performing a stable update for other observation depths could not be identified.

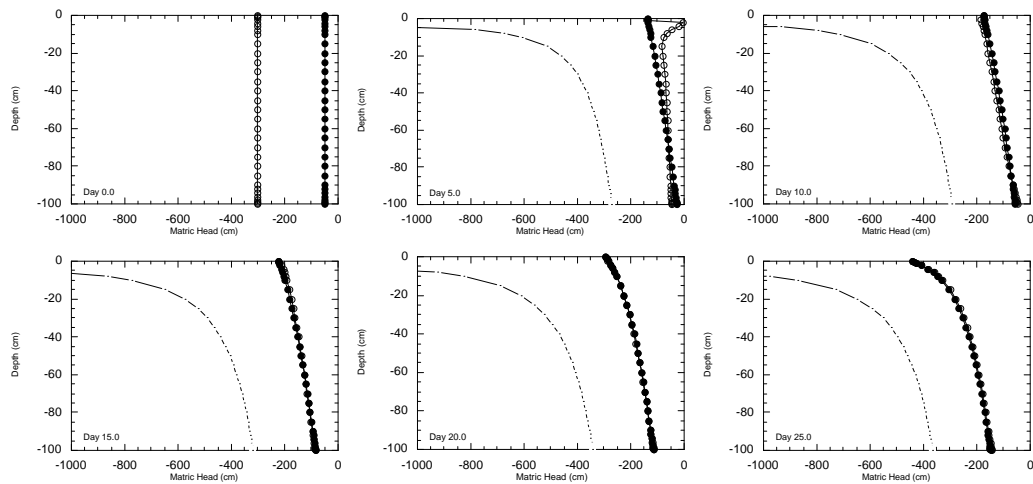


Figure 6.47: Comparison of soil moisture profile estimation using the Kalman-filter assimilation scheme for an observation depth of 1 cm and log transformation (open circle) with the “true” soil moisture profile (solid circle) and the open loop soil moisture profile (open circle with dot); initial state variances 1000000, observation variances 2% of observations and system noise 15% of states per hour.

6.4.4.2.6 Volumetric Moisture Transformation in the Kalman-Filter

Whilst the log transformation reduced the difference between the observations and model predictions of near-surface soil moisture, the transformed soil moisture profile maintained the large gradient of matric head with depth near the soil surface. However, the corresponding volumetric soil moisture profile does not exhibit this same property (Figure 6.48), as volumetric soil moisture content is constrained by the residual soil moisture content and the soil porosity. Thus, a volumetric soil moisture transformation reduces the difference between observations and model predictions, as well as the non-linearities in the shape of the soil moisture profile, particularly in the vicinity of the near-surface observations. Thus, the non-linearities in the ψ -based model used in PROXSIM1D (Chapter 5), which are believed to be the cause of the extended Kalman-filter updates diverging from the “true” soil moisture profile, are reduced by using a θ -based model.

The transformation of the model soil moisture state from matric head to volumetric soil moisture content can be achieved by the water retention relationships in (5.44) to (5.46). However, the covariances of the model states must also be transformed into volumetric soil moisture space. This may be achieved by

$$\Sigma_Y = \mathbf{B}\Sigma_X\mathbf{B}^T \quad (6.4),$$

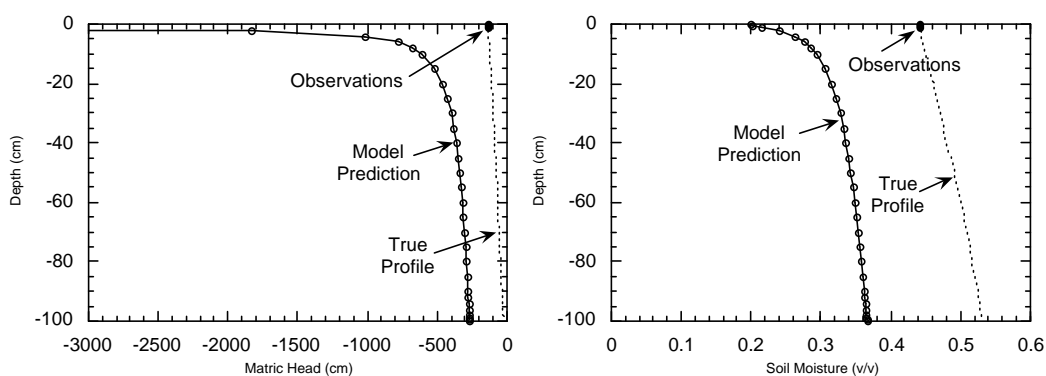


Figure 6.48: Illustration of the reduction in profile non-linearity by using a volumetric soil moisture transformation of the soil matric head.

where Σ_y is the covariance matrix of \mathbf{Y} (the transformed system) and Σ_x is the covariance matrix of \mathbf{X} (the original system), being the covariance matrix requiring transformation. For the general case of the system states ψ and T augmented with the system parameters α (see Appendix A), then

$$\mathbf{Y} = \begin{bmatrix} \theta_{l_1} \\ \theta_{l_2} \\ \vdots \\ \theta_{l_N} \\ \dots \\ T_1 \\ \vdots \\ T_N \\ \dots \\ \alpha_1 \\ \vdots \\ \alpha_N \end{bmatrix} \quad \mathbf{X} = \begin{bmatrix} \psi_1 \\ \psi_2 \\ \vdots \\ \psi_N \\ \dots \\ T_1 \\ \vdots \\ T_N \\ \dots \\ \alpha_1 \\ \vdots \\ \alpha_N \end{bmatrix} \quad (6.5).$$

The matrix \mathbf{B} is a transformation matrix given by

$$\mathbf{B} = \begin{bmatrix} \frac{\partial \theta_{l_1}}{\partial \psi_1} & \frac{\partial \theta_{l_1}}{\partial \psi_2} & \dots & \frac{\partial \theta_{l_1}}{\partial T_1} & \dots & \frac{\partial \theta_{l_1}}{\partial \alpha_m} \\ \frac{\partial \theta_{l_2}}{\partial \psi_1} & \frac{\partial \theta_{l_2}}{\partial \psi_2} & \dots & \frac{\partial \theta_{l_2}}{\partial T_1} & \dots & \frac{\partial \theta_{l_2}}{\partial \alpha_m} \\ \vdots & \vdots & \ddots & \vdots & \vdots & \vdots \\ \frac{\partial T_1}{\partial \psi_1} & \frac{\partial T_1}{\partial \psi_2} & \dots & \frac{\partial T_1}{\partial T_1} & \dots & \frac{\partial T_1}{\partial \alpha_m} \\ \vdots & \vdots & \vdots & \vdots & \ddots & \vdots \\ \frac{\partial \alpha_m}{\partial \psi_1} & \frac{\partial \alpha_m}{\partial \psi_2} & \dots & \frac{\partial \alpha_m}{\partial T_1} & \dots & \frac{\partial \alpha_m}{\partial \alpha_m} \end{bmatrix} \quad (6.6).$$

The relationship between \mathbf{Y} and \mathbf{X} is given by

$$\theta_{l_j} = f(\psi_j, \alpha) \quad (6.7a)$$

$$T_j = T_j \quad (6.7b)$$

$$\alpha_i = \alpha_i \quad (6.7c).$$

As the transformation of the system states at node j is independent of the system states at other nodes and the transformation of parameter i is independent of the other parameters, a diagonal matrix is obtained with zero on the off diagonal terms. The exception to this is the dependence of system states to the model parameters in the top right hand quadrant. Thus, the transformation matrix may be given by

$$\mathbf{B} = \begin{bmatrix} C_{\psi_1} & & 0 & & & \frac{\partial \theta_{l_1}}{\partial \alpha_1} & \dots & \frac{\partial \theta_{l_1}}{\partial \alpha_m} \\ & \ddots & & & 0 & \vdots & \ddots & \vdots \\ 0 & & C_{\psi_N} & & & \frac{\partial \theta_{l_N}}{\partial \alpha_1} & \dots & \frac{\partial \theta_{l_N}}{\partial \alpha_m} \\ \hline & & & 1 & 0 & & & \\ & 0 & & & \ddots & & 0 & \\ & & & 0 & 1 & & & \\ \hline & & & & & 1 & & 0 \\ & 0 & & 0 & & & \ddots & \\ & & & & & 0 & & 1 \end{bmatrix} \quad (6.8),$$

where C_{ψ} is the capillary capacity factor $\partial \theta \partial \psi$ given by (5.47) to (5.49) and $\partial \theta \partial \alpha$ are given by (A.39) to (A.49) of Appendix A. The re-transformation of the updated covariance matrix may be achieved by

$$\Sigma_x = \mathbf{B}^{-1} \Sigma_y \mathbf{B}^T \quad (6.9).$$

The problem associated with transforming the system states from matric head to volumetric soil moisture is the assumption of normality for the errors. That is, when the soil moisture content approaches the residual soil moisture content or the soil porosity, the Kalman-filter believes the standard deviation should be small, as soil moisture content cannot be less than the residual soil moisture content or greater than the soil porosity. What the Kalman-filter does not recognise is that the forecast soil moisture content could be much wetter in the dry case, or much drier in the wet case. The problem that this creates is that the

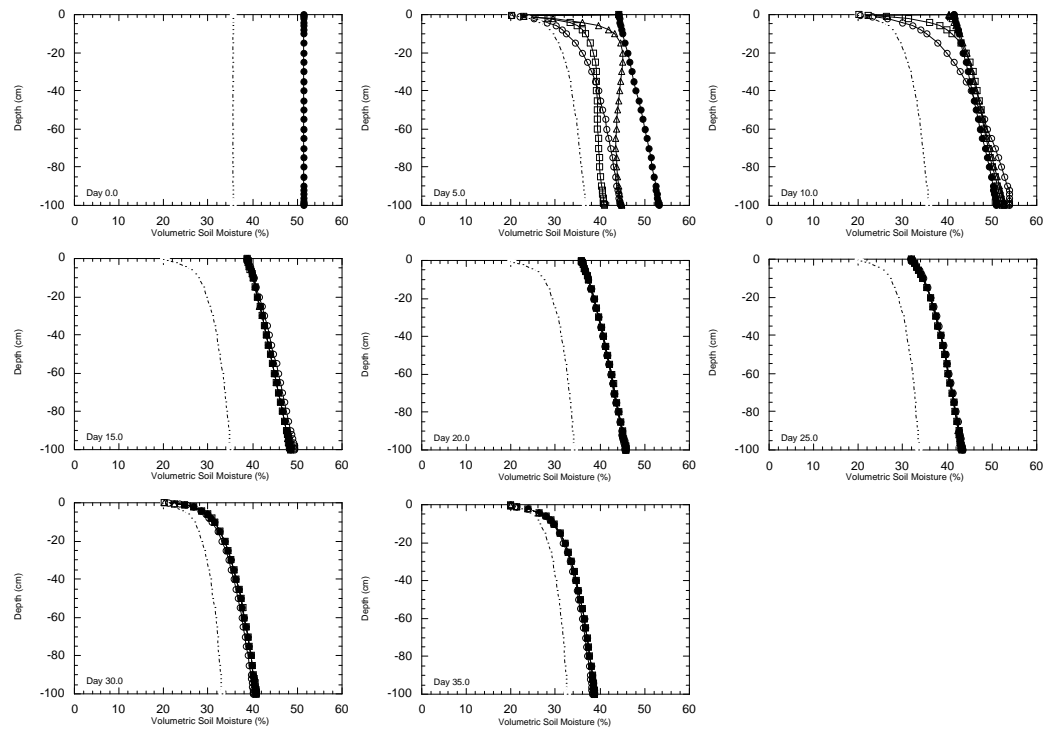


Figure 6.49: Comparison of soil moisture profile estimation using the Kalman-filter assimilation scheme for observation depths of 1 (open circle), 4 (open square), and 10 cm (open triangle) with the “true” soil moisture profile (solid circle) and the open loop soil moisture profile (open circle with dot); moisture transformation of states and state covariances. Initial state variances of 1000000, 10000 and 10000 respectively, observation variances 2% of observations and system noise 5% of states per hour.

Kalman-filter interprets these small standard deviations as a high degree of certainty in the model prediction and ignores the observation. To overcome this, a limit was placed on the minimum value for $\partial\theta\partial\psi$ to ensure that reasonably large standard deviations were maintained for the transformed system states near the soil surface, whilst ensuring that the standard deviation was not greater than the soil porosity. A value of $1e-6$ was used for this purpose.

Using this volumetric soil moisture transformation, stable soil moisture profile updates were obtained for all observation depths apart from the surface node. Stable updates could not be achieved for surface node observations, as the transformation process resulted in a low correlation with forecast soil moisture content at deeper depths. The results for simulations using the volumetric soil moisture transformation are given in Figure 6.49.

These results show that the “true” soil moisture profile was retrieved after 10 days for the 10 cm observation depth and 15 days for 1 cm and 4 cm observation depths. A larger initial state variance was used for the 1 cm

observation depth (1000000) than for the 4 and 10 cm observation depths (10000) to ensure that large standard deviations were obtained for near-surface nodes after the transformation. These profile retrieval results can be compared with those from the quasi observation simulations, which required 10 days for all observation depths. Only one extra update was required using the volumetric soil moisture transformation, and no assumption was required regarding the soil moisture profile. Furthermore, had soil moisture been the dependent state in the soil moisture model, retrieval of the “true” soil moisture profile may have been achieved more rapidly, as the transformation of covariances and its associated problems and assumptions would have been eliminated.

Hence, it would appear obvious that whilst the ψ -based form of the moisture equation is more correct in terms of modelling profile soil moisture for multi-layered soils, the θ -based form is required for stable updating with the Kalman-filter when observations and model predictions have a large departure. The reason for this is that the θ -based form of the moisture equation is more linear than the ψ -based form.

6.5 CHAPTER SUMMARY

It has been shown that the Kalman-filter assimilation scheme is superior to the continuous Dirichlet boundary condition and the hard-updating assimilation schemes, and that there is no improvement made to the estimate of the soil moisture or temperature profile through making hard-updates of the surface nodes alone. A summary of the simulation times required for retrieval of the “true” soil moisture and temperature profiles using the different assimilation schemes is given in Table 6.2, for the different observation intervals and soil moisture observation depths.

The superiority of the Kalman-filter comes through its ability to make adjustments to the entire profile, whilst hard-updates can only directly alter the profile within the observation depth. However, the Kalman-filter can only do this if there is a high correlation between the states of adjacent nodes. Thus, the model used for forecasting of the system states must have a dependence on the system states of the adjacent nodes.

Table 6.2: Summary of soil moisture and temperature profile retrieval times from the synthetic study using hard-updating and Kalman-filtering, with various observation depths and update intervals.

	Hard-Updating					Kalman-Filtering				
	Soil Moisture				Soil Temperature	Soil Moisture				Soil Temperature
Observation Depth (cm)	0	1	4	10	Surface	0	1	4	10	Surface
Update Interval	Profile Retrieval Time (days)					Profile Retrieval Time (days)				
Continuous	8	8	7	5	>20					
1 Hour	>20	12	8	–	–	0.5	0.5	0.5	0.5	2
1 Hour ¹	–	>20	16	10	–	0.7	0.7	0.7	0.7	2
1 Day ²		>20	>20	>20	>20					
1 Day						3	3	3	3	6
5 Days ³		>40	>40	40	40					
5 Days ⁴						10	10	10	10	15
5 Days ⁵						–	10	–	–	
5 Days ⁶						–	15	15	10	

1. Gravity drainage and advection boundary condition at base of soil column
2. Dirichlet boundary condition at soil surface for 1 hour after update
3. Dirichlet boundary condition at soil surface for 1 day after update
4. Quasi observations applied to remainder of profile
5. Log transformation
6. Moisture transformation

Being unable to directly alter more than the observed soil moisture and temperature values using the hard-updating assimilation scheme created a soil moisture mass and heat energy balance problem, as the soil moisture mass and heat energy added during an instantaneous hard-update is restricted by the depth

of the observation. This surface information is transferred to deeper depths through the internal physics of the model (ie. infiltration/exfiltration). Thus, an increased observation depth was an obvious advantage for the hard-update assimilation scheme. As the observations became less frequent, the hard-update assimilation scheme required a Dirichlet boundary condition, which had to be applied for an increasingly longer proportion of the update interval. This indicated that more frequent observations are more useful for profile estimation than knowledge of the surface states for a greater period of time.

The soil moisture mass and heat energy added during a continuous Dirichlet boundary condition is constrained by the physical rate at which soil moisture and heat can be transferred through the soil profile, and the length of time for which the Dirichlet boundary condition is maintained. Thus, observation depth had a reduced influence on the soil moisture and temperature profile retrieval time when the Dirichlet boundary condition was applied.

It has also been shown that observation depth did not have a significant effect on the “true” soil moisture and temperature profile retrieval time for the Kalman-filter assimilation scheme. However, it was observed that unrealistic updating of the profile occurred with the Kalman-filter when observations become less frequent, the observed and modelled profiles were far apart, and there was a large uncertainty in the modelled profiles. This again highlighted the importance of frequent observations, and suggested that for the Kalman-filter assimilation scheme, that repeat coverage frequency is more important than observation depth.

Whilst stable updating of the soil moisture profile using the Kalman-filter assimilation scheme was achieved by applying quasi observations for the unobserved portion of the moisture profile, this was undesirable and the usefulness of this approach was not widely verified. However, it has been shown that the Kalman-filter assimilation scheme was less susceptible to unstable updates if volumetric soil moisture was modelled as the dependent state, as this reduced the non-linearities in the soil moisture model. This is a key outcome of the synthetic study, as it has given invaluable insight relating to the model structure requirements for the spatial problem.

This synthetic study has shown that to estimate soil moisture profiles using the water balance approach, an assimilation scheme that has the non-mass conservative characteristics of the Kalman-filter is essential for efficient updating of the soil moisture and temperature profiles. Moreover, when using an assimilation scheme having this characteristic, the retrieval of “true” soil moisture and temperature profiles was insensitive to observation frequency and observation depth, providing a linear form of the forecasting model was used